UNIVERSITA' DEGLI STUDI DELLA TUSCIA DI VITERBO

DIPARTIMENTO PER L'INNOVAZIONE NEI SISTEMI BIOLOGICI, AGROALIMENTARI E FORESTALI (DIBAF)

CORSO DI DOTTORATO DI RICERCA

IN ECOLOGIA FORESTALE – XXV CICLO

CANOPY PROPERTIES ESTIMATION IN DECIDUOUS FORESTS WITH DIGITAL PHOTOGRAPHY

AGR/05

COORDINATORE: Prof. Paolo De Angelis

TUTOR : Dott. Andrea Cutini

DOTTORANDO : FRANCESCO CHIANUCCI

Acknowledgments

Ringrazio innanzitutto il Prof. Paolo de Angelis e il dott. Andrea Cutini, che mi hanno dato l'opportunità di perfezionare la mia formazione con il dottorato. Sono riconoscente al dott. Craig Macfarlane (CSIRO) per i preziosi consigli che mi ha fornito in fase di analisi e stesura del lavoro. Un sentito ringraziamento va anche al personale del CRA – SEL di Arezzo, in particolare a Umberto Cerofolini, Tessa Giannini, che mi hanno aiutato nello svolgimento dei rilievi in campo. Un ulteriore aiuto in campo mi è stato fornito anche da Giovanni Vagnoli e Giovanni Venturi, che qui ringrazio. Un grazie speciale va a mia moglie Alessandra, che mi ha sostenuto ed incoraggiato durante questi anni, e ai miei figli Pietro e Marta.

Hic tamen hanc mecum poteras requiescere noctem fronde super viridi: sunt nobis mitia poma, castaneae molles, et pressi copia lactis; et iam summa procul villarum culmina fumant, maioresque cadunt altis de montibus umbrae.

Virgilio, I Bucolica

Summary

Abstract

Rapid, reliable and meaningful estimates of forest canopies are essential to the characterization of forest ecosystems. The aim of the research was to conduct a thorough technical appraisal of existing available digital photographic methods for forest canopy estimation. The the more traditionally used digital hemispherical photography (DHP), which measures the gap fraction at multiple zenith angles, was compared with methods that measure the gap fraction at a single zenith angle, namely 57° photography and cover photography (DCP). DCP is a more recent canopy photographic method, which measures gap fraction at the zenith (0°).

These methods were applied in deciduous forests of beech, chestnut and Turkey oak. All photographic methods provided good indirect estimates of canopy properties, as compared with reference direct methods obtained by littertraps and AccuPAR ceptometers. However, all methods showed different advantages and disadvantages, which were discussed and addressed.

Among the methods, DCP showed high potential as a means to quickly obtain inexpensive estimates of forest canopy over large areas, being therefore highly suitable for routine, research and monitoring of forest canopy attributes. The method also appeared particularly suitable for calibrating nadir remotely-sensed canopy estimates, on account of its high vertical resolution imagery.

Comparison of logarithm gap fraction averaging procedures implied in DHP allowed defining a protocol for effective leaf area index and apparent clumping index extraction from non segmented analysis of gap fraction, which can be applied to both DHP and LAI-2000 PCA. The results have important implications for the evaluation of satellite-based leaf area index product of airborne laser scanning (LiDAR).

Comparisons of compact (point-and-shoot) cameras with digital single lens reflex cameras allowed defining standardized field protocol for image acquisition and software analysis. The outcome can greatly assist canopy photographic methods to achieve the standards of an ideal device.

The study also provided a suite of several variables of interest such as light extinction coefficient and crown porosity, which can provide insights towards the characterization of deciduous forests, and which can be further applied for further canopy studies in deciduous stands.

Keywords: Hemispherical photography, Cover photography, Leaf area index, Clumping, Light transmittance, Littertraps, LAI-2000, AccuPAR ceptometer.

1. Introduction

1.1 Background

A key aspect in characterizing forest ecosystems is obtaining accurate and reliable estimates of forest canopy (Chen et al. 1997). Leaves and crown are the active interface of energy, carbon and water exchanges between plant and atmosphere (Jarvis and Leverenz 1983). For this reason, crowns and canopy are more sensitive and react more promptly than other stand structural components to abiotic as well as biotic disturbances, and thus show effective potential for use in monitoring the status of forest ecosystems and establishing long-term research programs (Cutini 2003, Macfarlane 2011).

Among the properties, leaf area index (LAI) and photosynthetically active radiation (PAR) are key parameters to wide range of studies including hydrology, carbon and nutrient cycling, and global change (Macfarlane et al. 2007c). Consequently, the description of plant canopies and their interception of radiation have been the subject of considerable scientific endeavour involving both experimental and modelling investigations (Jennings et al. 1999; Van Gardingen et al. 1999). Despite the importance of these variables, it is very difficult to gain accurate and meaningful estimates of them.

Over the last few decades, much attention has been given to indirect estimates of forest canopy properties using ground-based instruments (Bréda 2003; Jonckhhere et al. 2004). This approach is mainly motivated because direct measurements are so destructive, expensive and time consuming that they are unsuitable for most forestry purposes (Jennings et al. 1999). By contrast, remotely sensed vegetation indices show novel potential, but still need site- and stand-specific calibration against ground-based measurements (Bréda 2003).

Indirect optical methods infer LAI and other canopy properties, such as forest light regime, by measurements of radiation transmission through the canopy and making use of radiative transfer theory (Ross, 1981). Among the methods, use of Licor LAI-2000 Plant Canopy Analyzer (PCA; Lincoln Inc., NE, USA) and of AccuPAR Ceptometer (Decagon Devices, Pullman, WA, USA) has gained wide acceptance for estimating LAI and light trasmittance in forest stands, respectively. Regardless of technical drawbacks related to these methods, a significant obstacle to their widespread adoption is represented by the high cost of the instrumentation (Macfarlane et al. 2007c).

Digital photography is a cost-effective and readily available alternative. Since the ’60s, film photography has been used for a long time in forest ecology. However, because it involved many time-consuming steps, it was progressively forsaken (Bréda 2003). More recently, advances in

digital photographic technology have led to a resurgence of interest in photography for indirect quantifying forest canopy. Digital cameras have greatly simplified image capturing and software processing, as compared with film cameras (Macfarlane 2011).

Among the techniques, digital hemispherical photography (DHP), also known as fisheye photography, has long been the most frequently employed of several photographic techniques for describing forest canopies. Hemispherical photography provides estimates of canopies via photographs acquired through a fisheye lens from beneath the canopy oriented towards the zenith (Jonckheere et al. 2004). Hemispherical photography measures the gap fraction at multiple zenith angles; it is characterized by an extreme angle of view, generally with a 180° field of view. The method is cost-effective, as it uses standard camera with a fisheye lens. Nevertheless, the sensitivity of outputs to photographic exposure and image processing is a major drawback (Cescatti 2007; Jonckheere et al. 2004; Zhang et al. 2005). Accordingly, strict protocol should be developed to prevent problems from compounded errors (Jonckheere et al. 2004).

More recently, a new digital photographic technique was proposed by Macfarlane et al. (2007c) namely digital cover photography (DCP). The method involves collecting vertically oriented digital photographic images with a narrow field of view (roughly 30°) and dividing the total zenithal gap fraction into between-crowns and within-crown gaps (Pekin and Macfarlane 2009). The method was pioneered in sparse canopies of *Eucalyptus* stands in Australia (Macfarlane et al. 2007c) and then it was successfully applied in sparse canopies of *Populus euphratica* stands in China (Zhongguo et al. 2009) and in an open savanna ecosystem in California (Ryu et al. 2010b). DCP has the advantage that it can be applied during normal working hours due to its insensitivity to photographic exposure, unlike DHP and PCA. The method provides several canopy properties aside from LAI, such as canopy (crown and foliage) cover, crown porosity and zenithal clumping index; however, the method requires an assumed zenithal extinction coefficient to estimate LAI. As another alternative to fisheye and cover photography, use of single direction view photography pointed at 57.5 degree angle provides LAI values without knowledge of the extinction coefficient, because the extinction coefficient is largely independent of the foliage angle distribution at this zenith angle. So far, LAI estimated from both 57.5 degree and DCP has been evaluated directly only in forest stands with low LAI values (< 3.0 m^2m^{-2}); thus, a thorough appraisal in more dense canopies is strongly required.

The aim of the current research is to evaluate digital photographic methods for the estimation of canopy properties in dense deciduous forests. The study mainly focussed on LAI; however, since leaf area is computed by other important canopy structure variables such as leaf angle and foliage clumping, other canopy traits retrievable from photography were analyzed and their reliability was discussed.

1.2 Problem definition

Indirect optical methods such as digital photography are based on measurements of the radiation transmission through the canopy. These methods apply the Beer-Lambert law taking into account that the total amount of radiation intercepted by a canopy layer depends on incident irradiance, canopy structure and optical properties (Monsi and Saeki 1953); this approach requires the assumption that all foliage elements are randomly arranged within the canopy. It is well-accepted that the main source of error in indirect optical LAI estimation (and other related canopy properties) is a result of canopy's deviation from the random assumption, which was named clumping (Bréda 2003; Chen et al. 1997; Jonckheere et al. 2004; Macfarlane et al. 2007c, Ryu et al. 2010a).

With the available technology, digital photography is able to provide clumping indices (Ω), to accurately estimate LAI from analysis of gap fraction distribution and/or gap size distribution, thereby producing information on the spatial distribution of leaves. However, since clumping effects appear at multiple scales from within-crown level to between-crowns level (Kucharik et al. 1997; Ryu et al. 2010b), different methods quantifying distinct scales of clumping might results into different Ω values. So far, the clumping indices from digital photography have been calculated only in sparse forest canopies, which were characterized by higher between-crowns clumping than within-crown clumping (Leblanc et al. 2005, Macfarlane et al. 2007c). Moreover, Ryu et al. (2010a) recently proposed a method to calculate clumping effects at between-crowns level with the LAI-2000 PCA, which can be implemented in fisheye photography; this approach was successfully tested in a sparse and heterogeneous savanna ecosystem in California. Nevertheless, the degree of clumping in dense canopies and the resulting accuracy of clumping indices calculated from optical methods in dense deciduous forests is still open to debate.

Another source of discrepancy from optical methods is the need to know the foliage angle distribution (Chen and Cihlar 1995). DHP automatically estimates the foliage angle distribution by measuring gap fraction at multiple zenith angles. 57.5 degree photography instead assumes LAI is insensitive to foliage angle at that angle. By contrast, DCP requires a zenithal light extinction coefficient, which is most dependent on leaf inclination angle. However, the reliability of these approaches has been rarely investigated.

Another source of discrepancy is because of the contribution of the supporting woody materials to the radiation interception measurement. Accordingly, all indirect optical methods estimate a Plant Area Index, because they include the contribution of woody elements (Bréda 2003; Chen and Cihlar 1995).

In addition to these, specific technical limitations arise, when using digital photography. A great drawback of photographic methods for estimating canopy metrics has been the tedious and time consuming image processing step and the perceived sensitivity of the results to image processing (Jonckheere et al. 2004, Macfarlane 2011). The sum of these factors may results in different canopy estimates.

1.3 Research objectives

The aim of the study is to assess the accuracy of digital photography for estimating canopy properties in dense deciduous forests, using the more traditional DHP - which has a long history of application in forestry and plant ecology (Evans and Coombe 1959; Anderson 1964) – with the more recently developed DCP. Another technique derived from DHP, namely 57.5 degree photography (Bonhomme et al. 1974) was also tested. Forest stands of the most common deciduous species in Italy, which differed in age, stand structure and silvicultural treatment, were analysed. Other indirect methods commonly used to estimate canopy properties, such as LAI-2000 PCA and AccuPAR ceptometer were also tested, to compare the performance of digital photography with other canopy instrumentations.

The specific objectives of the study were:

- To evaluate the accuracy of LAI from digital photography, as compared with direct LAI derived from litterfall, a direct approach which was considered the most precise method in deciduous forests (Chen et al. 1997; Dufrêne and Bréda 1995);
- To evaluate the accuracy of light estimates from DHP with direct measures from AccuPAR ceptometer, obtained in different sky conditions;
- To assess strength and weakness of the different methods, in order to propose corrective strategies to overcome some technical drawbacks of the different photographic techniques;
- To compare and evaluate different gap fraction averaging approaches applicable in DHP and PCA, and the resulting different clumping indices obtainable, and to test the accuracy of the different approaches;
- To conduct a thorough technical appraisal between digital point-and-shoot-cameras- which have been more frequently employed in forestry and plant ecology- and more recent higher quality digital single-lens-reflex (DSLR) cameras.

2. Literature and Theory review

2.1. Canopy definition and units of canopy structure

Canopy is the combination of all leaves, twigs, and small branches in a stand of vegetation; it is the aggregate of all crowns; the open spaces (gap fraction) between canopy elements and the atmosphere contained within- and between-crowns were considered as part of the canopy (Lowman and Nadkarni 1995). Canopy structure is the organization in space and time of these aboveground components of vegetation (Norman and Campbell 1989).

Because measuring all leaves or twigs in a forest canopy is unrealistic, canopy structure can be measured at several levels of detail. It is most commonly described by a characteristic descriptor, such as tree height, stocking rate, canopy cover, and light trasmittance. However, leaf area index is the variable most commonly used to quantify forest canopy.

2.2. Definitions of LAI

Leaf area index is a dimensionless variable and was first defined as the total one-sided area of photosynthetic tissue per unit ground surface area (Watson 1947). For broad-leaved species with flat leaves, this definition is easily applicable (Jonckheere et al. 2004). For non flat leaves (i.e., coniferous leaves), this approach in no longer feasible (Chen and Black 1992). Some authors proposed a projected leaf area to overcome the problem of irregular form of needles and leaves (Smith 1991). Myneni et al. (1997) also proposed the maximum projected leaf area per unit ground surface area. By contrast, Lang et al. (1991) and Chen and Black (1992) suggest half the total interception area per unit ground surface area would be more adequate for non-flat leaves, because they criticized the physical and biological significance of the projected area concept. Different definitions of LAI were also proposed subsequently.

In the current literature and close to Watson's definition, the following definition has gained wide acceptance: LAI is one half the total leaf area per unit ground surface area (Chen and Black 1992).

2.3 Ground-based methods for LAI determination

There are two main categories of procedure to estimate LAI: direct and indirect methods. Direct methods measure LAI in a direct (or semi-direct, see Dufrêne and Breda 1995) way, while

indirect methods derived LAI from measurements of related variables. In the next section the description of the methods were presented.

2.3.1 Direct methods

Direct methods are the most accurate, but they have the disadvantage of being time-consuming and as a consequence making broad scale application not feasible (Jonckheere et al. 2004). Accordingly, these methods are not suitable for routine measure and monitoring of LAI and other forest canopy properties. However, the need for validation of indirect and remotely sensed methods remains, so direct methods can be considered important as cross-calibration tools (Cutini et al. 1998).

Direct methods involve measurement of leaf area, using either a leaf area meter or a specific relationship of dimension to area via a shape coefficient (Bréda 2003). In coniferous species, projected leaf area differs from the developed one by a coefficient depending on a needle cross-section area (Grace 1987, Barclay 1998, Sellin 2000). Leaf area is determined through repeated area measurements on single leaves and area accumulation (Jonckheere et al. 2004).

Harvesting of trees for direct measurement is the most accurate method, but it is labour intensive, time-consuming and destructive, and practical only in small areas (Bréda 2003, Macfarlane et al. 2007c). This method is better suitable for vegetation of small structure, such as crops and pastures, but is unrealistic in forest stands.

One less destructive method using allometry has been frequently applied in forested ecosystems. This method enables estimation of LAI by measurement of more readily acquirable variable such as diameter at breast height or total height. However, this method is destructive, tedious and time-consuming, and not immune of error because is it site- and species-dependent (Bréda 2003).

In deciduous forests, the litterfall method is a non-destructive direct method consisting of collecting leaves in traps distributed below canopy during leaf-fall period. The litterfall method provides an integrated measure of LAI over the whole measurement period, not at a single moment in time during the growing season. The method is reliable for deciduous species, in which the total leaf fall is directly related to the maximum LAI. For some species which can replace their leaves during the growing season, such as poplar, the method overestimates the maximum LAI (Jonckheere et al. 2004). Additional source of errors may results from SLA estimation; however, this method is less laborious and time consuming than the other direct methods and is the only one giving access to the contribution of each species to total leaf area index (Bréda 2003). Once again, this method is considered the most precise one for deciduous forests. (Dufrêne and Bréda 1995).

2.3.2 Indirect methods

Indirect methods infer leaf area index, and other canopy properties, from measurements of the transmission of radiation through the canopy and making use of the radiative transfer theory (Ross 1981). These non-destructive methods are based on a statistical and probabilistic approach to foliar element (or its complement, gap fraction), distribution and arrangement within the canopy (Bréda 2003). LAI is calculated by inversion of the Beer-Lambert law, which computes canopy transmittance (Equation (1)):

$$P(\theta) = \exp\cdot\left(-\frac{G(\theta,\alpha)LAI}{\cos(\theta)}\right) \quad (1)$$

Where P(θ) is the gap fraction at a given zenith angle (θ), α is the leaf angle, G(θ) is the G-function and correspond to the fraction of foliage projected on the plane normal to the zenith direction. G-function depends from θ and leaf angle α, but the latter is generally unknown.

Bréda (2003) proposed a distinction between gap fraction-based and radiation measurement methods. Jonckhere et al. (2004) instead proposed a distinction between instruments based on gap fraction analysis and instruments based on gap size distribution. However, these classifications are unable to provide a clear distinction between fisheye photography and cover photography; as such, in this study optical indirect methods were divided into two main categories: a first group contains instruments based on multiple zenith angle measurements of gap fraction, while a second group contains instruments based on single zenith angle measurement of gap fraction, similarly with the classification provided by Weiss et al. (2004). This is mainly desirable because different approaches provide different measures of forest canopy and traditional classification may lead to considerable confusion over what is really measured. Jennings et al. (1999) reported a useful discussion of the sometimes confusing terminology relating to canopy measurements in forest vegetation.

Methods based on multiple zenith angle measurements compute LAI by inversion of equation (1):

$$LAI = -\frac{\ln[P(\theta)]\cos(\theta)}{G(\theta)} \quad (2)$$

Equation (2) is independent from leaf angle (α). Hemispherical photography and LAI-2000 PCA are the most commonly used methods based on multiple zenith angle measurements.

Originally, methods based on single zenith measurement were radiation measurement methods; LAI is computed by measurement of both incidence irradiance (I) and below-canopy radiation (I_0), assuming a random distribution of leaves within the canopy (Equation (3)):

$$I = I_0 \exp(-kLAI) \quad (3)$$

Where k is the extinction coefficient. By combining eq. 2 and 3, the expression for k is (Equation (4)):

$$k(\theta, \alpha) = G(\theta, \alpha) / \cos(\theta) \quad (4)$$

As such, the extinction coefficient is dependent from zenith angle and leaf angle. Methods involving ceptometer and cover photography are both based on single direction view measurement of trasmittance at the zenith (0°); under certain assumptions (see below), gap fraction from cover photography is the equivalent of transmittance from ceptometer. Another method based on single direction measurement is 57.5° view angle photography, which is a method derived from fisheye photography. Use of 57.5° (≈ 1 radian) is desirable because at that zenith angle both the G-function and the extinction coefficient are almost independents from leaf angle (G~ 0.5; k~0.91; Warren and Wilson 1963); Bonhomme et al. (1974) used 57.5° view angle of hemispherical images to estimate LAI in young crops.

All indirect optical methods share the following assumptions:

- Leaves are randomly distributed within the canopy;
- Leaves are small compared to the total field of view of the sensors and compared with the canopy;
- Foliage is black, namely leaves do not transmit light.

Under these assumptions, gap fraction and transmittance are equivalent (Bréda 2003).

2.4 Canopy instrumentation

2.4.1 Digital photography

Photography can be thought of as “upside down” remote sensing. Among the techniques, hemispherical photography has a long history of application in forestry and plant ecology and has been the subject of several reviews (Chen et al. 1997, Kucharik et al. 1999, Bréda 2003, Jonckheere et al. 2004, Weiss et al. 2004, Chianucci and Cutini 2012). In the following sections an overview of the available digital photographic methods to estimate canopy properties are presented.

2.4.1.1 Multidirectional view photography: hemispherical photography

Hemispherical images are acquired via a film or digital camera fit with a fisheye lens from beneath the canopy and oriented towards the zenith. Hemispherical photography has an extreme angle of view (180° FOV). The fisheye image provides a permanent record of sky and vegetation geometry, which is used to calculate solar radiation regimes and canopy properties such as LAI and openness (Rich et al. 1999; Figure 1).

Hemispherical photography is a method that measures the gap fraction at multiple zenith angles. Gap fraction is computed by applying the Beer-Lambert law, modified for clumping effects by Nilson (1971), Equation (5):

$$P(\theta) = \exp\left(-\frac{G(\theta)\Omega(\theta)LAI}{\cos(\theta)}\right) \quad (5)$$

Where Ω(θ) is the clumping index at a given zenith angle; LAI is the leaf area index including leaf and woody materials (also called Plant area index - PAI; Bréda 2003) . Clumping indices can be calculated from an analysis of the gap size distribution (Chen and Cihlar 1995), the gap fraction distribution (Lang and Xiang 1986), or combining both the gap size and the gap fraction distribution analysis (Leblanc 2002).

Measuring the gap fraction at multiple zenith angles enables estimation of both LAI and foliage angle distribution simultaneously, thus avoiding the need to known *a priori* the extinction coefficient (which is related to the G-function). Hemispherical photography has been also used to estimate the percentage of incident photosynthethic photon flux density (PPFD) transmitted through gaps (Canham et al. 1990).

2.4.1.2 Current controversies and opportunities of hemispherical photography: an overview

The first fisheye lens was developed by Hill (1924) to study cloud formation. Later, the first approach to fisheye photography in forestry was provided by Evans and Coombe (1959), which used hemispherical photography to describe the light environment under forest canopy. Anderson (1964 and 1971) used fisheye photography to calculate the direct and scattered components of solar radiation from visible sky directions. Subsequently, film hemispherical photography has been used for a long time to estimate forest canopy properties (Bonhomme et al. 1974, Anderson 1981, Chan et al. 1986, Wang and Miller 1987). However, technical and theoretical obstacles involving many

time consuming steps have progressively prevented wide spread adoption of film hemispherical photography (Bréda 2003, Macfarlane et al. 2007b).

Hemispherical Image
~180° FOV
Medium resolution
Poor vertical sampling
Large effective plot size per image

57.5 degree image
~60° FOV
Low resolution and small number of pixels
No vertical sampling
Medium effective plot size per image

Cover image
~30° FOV
High resolution
Mainly vertical sampling
Small effective plot size per image

Figure 1 - Comparison of digital photographic images

More recently, advances in digital photographic technology and image processing software have led to a renewal of interest in digital hemispherical photography for indirect quantification of forest canopy properties (Bréda 2003, Macfarlane et al. 2007b, Jarčuška et al. 2010). Digital cameras have greatly simplified the process of image capture and processing, when compared with film cameras (Macfarlane 2011). In addition, over the last few years, numerous commercial software packages, as well as freeware programs for canopy analysis, have been developed (Frazer et al. 1999, Jonckheere et al. 2005, Jarčuška 2008).

In spite of these recent improvements, a significant obstacle to widespread adoption of digital hemispherical photography (DHP) remains, that of automation of the analysis of canopy images, which is tedious and time consuming (Jonckheere et al. 2004). Moreover, the sensitivity of outputs to camera exposure and image processing (in particular, gamma correction, thresholding) is a major drawback (Jonckheere et al. 2004, Cescatti 2007). The importance of exposure control is well documented, since automatic exposure has been demonstrated to prevent accurate and reliable estimates of the gap fraction (Chen et al. 1991, Macfarlane et al. 2000, Zhang et al. 2005). Images taken with automatic exposure underestimates gap fraction in open canopies, while overestimates gap fraction in medium-high density canopies (Zhang et al. 2005); as a consequence, exposure needs to be manually set.

Gamma function is another source of uncertainty for hemispherical imagery. The gamma function describes the relation between actual light intensity during photography and the resulting brightness value of the pixel (Wagner 1998). A gamma value of 1.0 denotes an image that accurately reproduces actual light intensity (Macfarlane et al. 2007b). Digital cameras typically have gamma values between 2.0 - 2.5. The main effect of this correction is to lighten the midtones, thus resulting in worse estimate of canopy light transmittance (Cescatti 2007).

Even though an apparent advantage of fisheye photography is that LAI and the extinction coefficient (k) are simultaneously estimated (Equation 4), previous studies found that the foliage angle distribution calculated from hemispherical photography appeared sensitive to canopy structure (Chen and Black 1991, Macfarlane et al. 2007a). As such, the foliage angle distribution calculated from fisheye images should be treated with caution.

2.4.1.3 Unidirectional view photographic methods: 57.5 degree and cover photography

To overcome the main drawback of hemispherical photography, that of the high and skilled intervention of the operator on canopy image analysis needed, different photographic approaches and procedures have been alternatively proposed. Among these, single-direction view photographic methods are theoretically simple and convenient, and have many advantages over fisheye photography. For example, digital photography taken at vertical and restricted field of view

provides better spatial resolution than the corresponding hemispherical photography (Pekin & Macfarlane 2009). In addition, unidirectional view photography methods are quite insensitive to light conditions and camera exposure (Macfarlane et al. 2007a).

The disadvantage of single direction gap fraction measurement methods is the extinction coefficient needs to be known a priori, unlike methods based on multiple gap fraction measurements such as fisheye photography. It can be determined experimentally from independent destructive measurements of leaf area index (Macfarlane et al. 2007a) or by deriving leaf inclination angle from levelled-digital camera approach (Ryu et al. 2010b; Pisek et al. 2011).

A different approach has been proposed using 57.5 degree photography. The method was derived from the inclined point quadrat method by Warren-Wilson (1960). The rationale behind this method is that for a view angle of 1 radian (57.5°) the G-function can be considered almost independent of leaf inclination (G~0.5; k~0.91; Equation (6)):

$$LAI = -\frac{\ln[P(57.5)]}{0.91} \tag{6}$$

In addition, the 57.5° approach implies that when foliage inclination angle is about 56°, G is insensitive to view angle θ. This angle approximately equals the mean foliage inclination angle of a spherical distribution model (de Wit 1965), which is a reliable approximation for several canopy types. The major obstacle of 57.5 degree photography is the potentially large contribution of woody area sampled in the image, which would limit the accuracy of canopy properties estimates.

As another alternative to fisheye photography, Macfarlane et al. (2007c) proposed digital cover photography (DCP), a method based on a single zenithal gap fraction measurement. Unlike fisheye photography, DCP uses a narrow field of view (approximately 30° FOV) by pointing a 70 mm (35 mm format equivalent) focal length lens upwards and achieves very fine spatial resolution (Figure 1; Macfarlane et al. 2007b, 2007c). This provides a compromise between vertical FOV and adequate spatial sampling, and is also comparable with the first ring of the LAI-2000 PCA. The DCP method divides gap into those where Beer-Lambert's law applies (within-crown) and those where it does not (between-crowns; Pekin and Macfarlane 2009). The method provides estimate of crown cover (% ground covered by the vertical projection of solid crowns) and foliage cover (% ground covered by the vertical projection of foliage and branches). The method has many advantages over fisheye photography. It is rapid and insensitive to exposure, and is able to provide several canopy properties, but requires an assumed zenithal light extinction coefficient (k) to estimate LAI.

A more detailed descriptions of the models used in DHP and DCP are provided in the materials and methods section; however, an useful distinction made by Jennings et al. (1999) between two basic types of canopy measurements is illustrated and described below, which allows to discriminate between the different photographic methods (Figure 2).

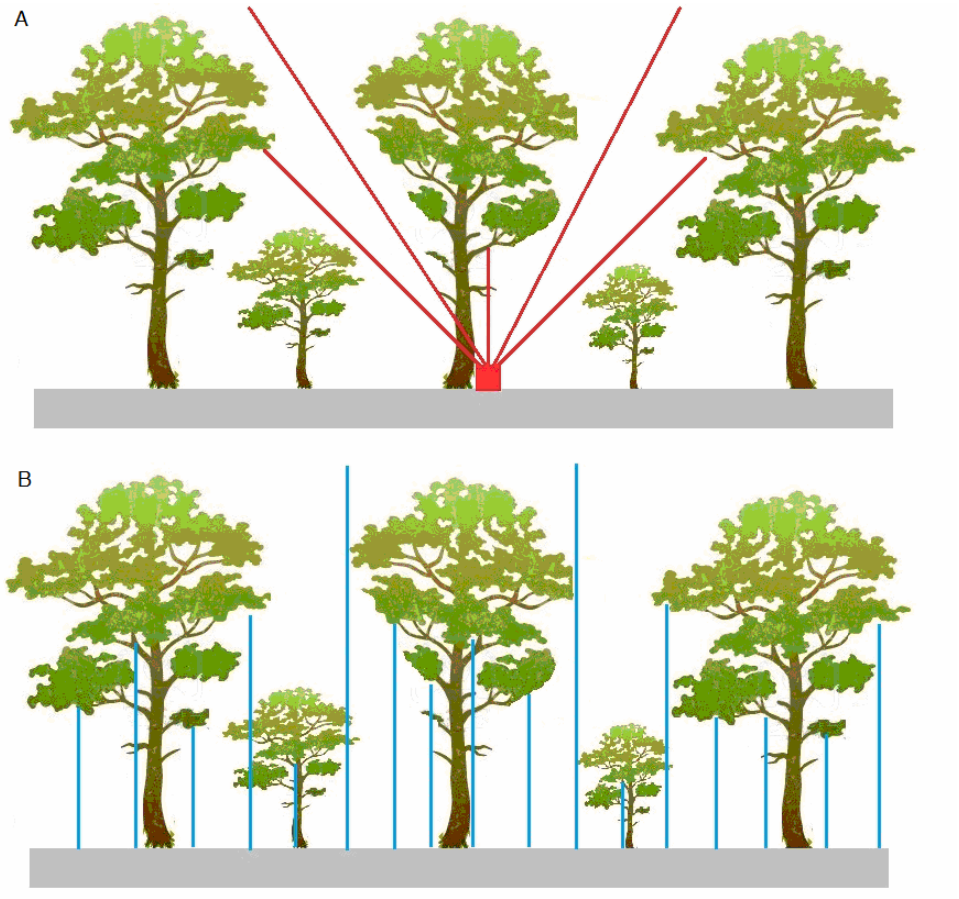

Figure 2 - Comparison of canopy closure (A) and canopy cover (B).

A) *Canopy closure* is the proportion of the sky hemisphere obscured by vegetation when viewed from a single point of view. Canopy density is a synonym often found in forestry literature. The term canopy openness is frequently used as the complement of canopy closure (Openness=1-canopy closure) and is defined as the proportion of the sky hemisphere not obscured by vegetation when viewed from a single point. Fisheye photography is a technique used to measure canopy closure.

B) *Canopy cover* refers to the proportion of the forest floor covered by the vertical projection of the tree crowns. This is analogous to the use of term cover. Cover photography is a technique that measure canopy (foliage and crown) cover.

2.4.2 LAI-2000 PCA

LAI-2000 PCA is based on measurement of diffuse radiation attenuation caused by canopy in the blue part of electromagnetic spectra. The method is based on multiple zenith angle measurements, and the theoretical background is similar to that used in hemispherical photography. The instrument (Figure 3) has a data logger and a sensor; the sensor consists of a fisheye lens (148° FOV), a mirror and an optical sensor divided into five concentric rings (with central zenith angles of 7°, 23°, 38°, 53°, 68° set by default, respectively). Measurements made above and below canopy are used to determine canopy light interception at 5 zenith angles, from which LAI is computed using a radiative transfer model. In particular, the PCA method calculated LAI by applying equation (2) as modified by Miller (1967), (Equation (7)):

$$LAI = 2\int_0^{\pi/2} -[\ln P(\theta)]\cos\theta \sin\theta d\theta \qquad (7)$$

LAI-2000 may be regarded as a convenient version of hemispherical photography because image processing is not required (Chen et al. 1997). For instance, PCA has an optical filter in the sensor, which rejects radiation above 490 nm (blue), because the foliage elements have a much lower reflectivity and transmittance in the blue region of the visible electromagnetic spectrum (which meet the 'foliage is dark' assumption, see section 2.3.2); in DHP a similar results can be obtained (more laboriously) by processing the blue channel of the image at adequate exposure setting.

Figure 3 - LAI-2000 Plant Canopy Analyzer (PCA)

However, when comparing with DHP (see equation 5), PCA is unable to provide clumping index (Ω). In fact, owing to design limitation, PCA can't divide the zenith rings into azimuth segments, unlike DHP (Lang and Xiang 1986). As a consequence, PCA assumes foliage elements were randomly distributed in azimuth (within each ring). However, Ryu et al. (2010a) noticed that for multiple samples, two different averaging methods can be applied to equation (7), namely $\ln \overline{P(\theta)}$ and $\overline{\ln P(\theta)}$, which can provide different LAI estimates. They proposed an apparent clumping index (Ω_{APP}) as calculated by the ratio of the two averaging gap fraction methods, even though this apparent clumping index considers only between-crowns clumping (namely the distance between two sample measurements). For further details, see chapter 5.

2.4.3 Quantum measures

Incident radiation is both a limiting and basic environmental factor for every organism. The crucial energy for photosynthesis is delivered by the electromagnetic spectrum between 400 and 700 nm, namely the Photosynthetically Active Radiation (PAR). Some part of this radiation is reflected directly by green leaves (roughly 6-12%), some part is absorbed and some is transmitted through the canopy. PAR is a key parameter in several physiological and biomass models (Amiro et al. 2000).

Figure 4 - AccuPAR ceptometer

Various methods have been used to quantify forest light environment and PAR. Ideally, light should be measured continuously in order to sample spatial and temporal variability of the light

environment. However, this is not practical for most research, and methods based on percent incident radiation have gained wide acceptance (Gendron et al. 1998). Among the methods, characterizing the light environment via instantaneous measurement of light transmission on sunny days has been very popular (Comeau et al. 1993, Brown and Parker 1994, Smith and Ritters 1994). By contrast, Messier and Puttonen (1995) proposed to estimate light environments in the understory via instantaneous diffuse light transmission on overcast days.

Instantaneous light measurements can be collected using an accuPAR ceptometer (Figure 4). This instrument consists of line quantum sensor making use of 80 individual sensors on a probe and control units. It strictly measures incident radiation and transmitted PAR (Bréda 2003). LAI is derived from canopy light interception using Equation (3); this approach, defined 'canopy transmittance' method (Cutini 1996), requires assumption about the light extinction coefficient (k). The method is based on single zenithal measure, and the theoretical background is similar to that used in DCP, even though clumping effects are not readily available from ceptometer measures (Lang and Xiang 1986).

3. Materials and methods

3.1. Study sites

The study was carried out in three different forested areas of Tuscany, central Italy, in order to sample forest stands of the most widespread deciduous species: Turkey oak (*Quercus cerris* L.), chestnut (*Castanea sativa* Mill.) and beech (*Fagus sylvatica* L.), which cover 11.6%, 9.2% and 11.8% of the total forested surface in Italy (Italian National Forest Inventory 2005; www.infc.it), respectively.

In the three forested areas (Figure 5), 10 stands were sampled in 2011 and 11 stands were sampled in 2012. The selected stands were drawn from a network of permanent research plots, which were established in previous studies (see below). Specifically, four stands of Turkey oak were sampled in Massa Marittima (43°08' N; 10°54' E), two stands of chestnut were sampled in Abbadia San Salvatore (42°51' N; 11°40' E) and four stands of beech and one stand of chestnut were sampled in Chiusi della Verna – Alpe di Catenaia (43° 59' N; 11°55' E). Species composition in each stand was pure.

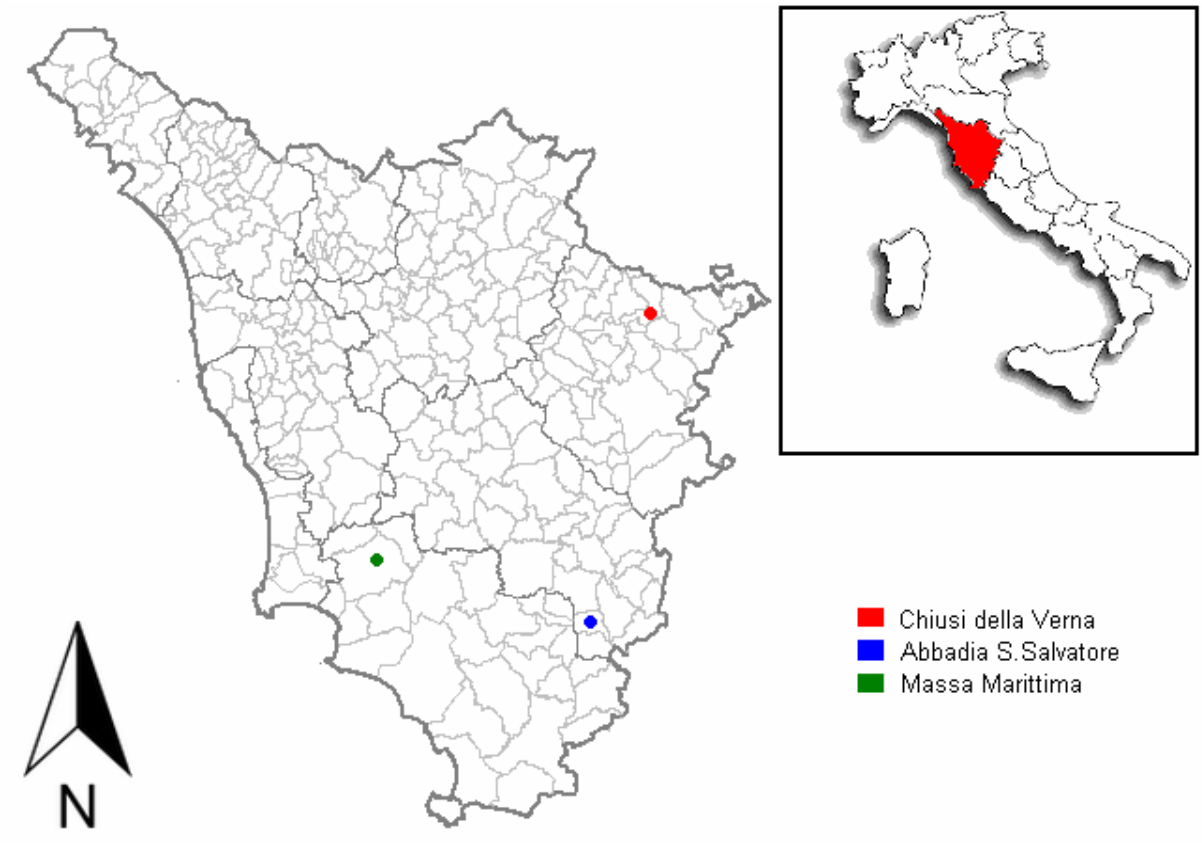

Figure 5 - Study area

The selected stands of Turkey oak consisted of experimental trials aimed at defining silvicultural option for management of oak coppices; the oak plots were located in Massa Marittima, within the 'Colline Metallifere' forested area. The area is an important oak vegetation area, where Turkey oak is the dominant species, but other different deciduous species were also present in minor percentage. In the past, the forested areas were mainly managed as coppices, due to charcoal for mine activity. The area is characterized by mild-Mediterranean climatic conditions. The mean annual rainfall was 906 mm (maximum concentration in autumn and spring), and the mean annual temperature was 14.4°C.

The selected stands of beech consisted of experimental trials aimed at defining management option for the conversion of ageing beech coppices into high forests (Amorini et al. 2009, Cutini et al. 2009). The study area for beech is located in the western slope of Alpe di Catenaia. The area (south-eastern Tuscany) well represents the typical forested ecosystems of central Apennines. Altitude ranged from 330 to 1,414 m a.s.l.. The climate was temperate, with hot and dry summers, and cold and rainy winters. The mean annual rainfall was 1,224 mm, and the mean annual temperature was 9.5°C. Roughly 87% of the mountainous area was covered in forests. Deciduous high forests, aged mainly between 50 – 70 years, were prevalent, while the rest consisted of deciduous coppices. The main species were beech, chestnut and Turkey oak. Additional stand of chestnut was selected within this study area in 2012.

The selected stand of chestnut consisted of experimental trials aimed at defining new management options for chestnut coppices (Amorini et al. 1998, Cutini 2001); the study area for chestnut is located in the eastern slope of Monte Amiata. Monte Amiata (1738 m a.s.l., south-western Tuscany) is an important chestnut vegetation area where, in the past, woods were traditionally coppiced every 8–10 years to obtain poles and posts for mine activity. Climate is mountain-Mediterranean: mean annual rainfall and temperature are, respectively, 1547 mm (maximum concentration in autumn and winter) and 10.0°C (hottest month +18.5°C, coldest month +1.8°C).

All the permanent plots were represented by ageing coppices in conversion into high forest, either by thinning or by natural evolution. When applied, thinning was selective and low; its grade was from light to heavy, with a temporary opening of the canopy cover (Cutini et al. 1998). Accordingly, the selected stands showed differences in age (29-66 years), stocking rate (108 – 4509 individuals ha^{-1}) and basal area (14.7 – 45.3 m^2), depending with the different silvicultural treatment applied. All the main stand characteristics of each plot were reported in Table 1.

Table 1 - Main stand characteristics of the studied stands

Species	Plot ID	Site	Elevation m. a.s.l.	Silvicultural treatment	Age years	Stems n ha^{-1}	Basal area m^2 ha^{-1}
Q. cerris							
	112	Massa Marittima	566	natural evolution	52	4509	30.2
	1324	Massa Marittima	568	1 medium thinning	52	3181	33.2
	2536	Massa Marittima	589	1 light thinning	52	4198	31.1
	3748	Massa Marittima	594	2 medium-heavy thinnings	55	402	21.2
F.sylvatica							
	TS	Chiusi della Verna	1080	seed cutting	67	108	14.7
	CONTR	Chiusi della Verna	1100	2 medium-heavy thinnings	67	419	34.6
	TEST	Chiusi della Verna	1050	natural evolution	67	3324	45.3
	DIR	Chiusi della Verna	1020	3 light-medium thinnings	67	414	23.8
C.sativa							
	DIR	Chiusi della Verna*	940	1 heavy thinning	62	920	37.6
	G2D	Abbadia S. Salvatore	870	2 medium thinnings	30	580	28.4
	G3D	Abbadia S. Salvatore	850	3 medium thinnings	30	447	23.9

* Stand added in 2012.

3.2. Field measurements

3.2.1 Direct measurements of LAI

Reference LAI values were directly estimated using litter traps ($LAI_{LT;}$ Figure 6). Cutini et al. (1998) described the procedure and accuracy of the method. In each plot, 9–15 litter traps were set out on a grid, at 1 m above ground level, with traps spaced 7–20 m apart, based on the stand homogeneity and structure. Litterfall was collected every 2 weeks in fall and winter 2011 and 2012, with the last collection timed soon after last leaf fall.

Figure 6 - Litter trap

Litter was sorted into its main components, and then dried for at least 24 h to a constant weight in a forced-air stove at 85°C ± 2° (Cutini et al. 1998). This method provides leaf dry mass per unit of ground area (g m^{-2}). Specific leaf area (SLA; cm^2 g^{-1}) was estimated from a sub-sample of about 200 leaves for each stand, with samples collected at every litterfall. The area of unwrinkled and undamaged leaves was measured with the Li-Cor 3000 area meter (Licor, Lincoln Inc., NE, USA), and the dry weight was measured.

The resulting SLA was corrected using a shrinkage coefficient (Vansereven 1969), which was estimated from a sub-sample of green leaves collected close to the research plots. Finally, the total dry mass of leaves collected was converted into LAI_{LT} by multiplication of the dry weight by the corrected SLA.

3.2.2 Direct measurements of canopy transmittance

Canopy transmitted light in the PAR waveband was measured during summer using AccuPAR ceptometer (Decagon Devices, Pullman, WA, USA). Instantaneous measurements of direct light were collected in summer 2011 and 2012 at midday on sunny days. Instantaneous diffuse light transmission was also measured close to sunrise or sunset in summer 2012, in order to measure different light components. Incident radiation was measured in open areas, which were located in the vicinity of the experimental plots. Below-canopy radiation was measured on a grid of 9–15 sample points, which were located within 2 m of the litter traps (Cutini 1996). For each sample point, four measurements at cardinal directions were recorded, averaged and stored in the instruments, for a total of 36–60 readings per plot. Transmittance was calculated as the percent fraction of below-canopy light divided by the incident radiation.

3.2.3 Estimates of canopy properties using digital photography

3.2.3.1 Camera setup, image acquisition and pre-processing of images

Digital images were first collected using the Nikon Coolpix 4500 compact camera (Figure 7); this is mainly desirable because the Nikon CoolPix models have been very popular in forest ecology, and the performance of these cameras have been deeply investigated (Leblanc et al. 2005, Zhang et al. 2005, Macfarlane et al. 2007c) . For instance, Frazer et al. (2001) compared film photography with the 2.1 Megapixel Coolpix 950; Inoue et al. (2004) compared the effect of quality and image size in two different Coolpix models (990 vs 900); Leblanc et al. (2005) used both Coolpix 990 and 5000 in boreal forests; Englund et al. (2000) tested the effect of image quality

using the Coolpix 950. These researchers found that little or no differences exists between TIFF and JPEG images from the same camera, but that image size can influence canopy properties estimates.

Figure 7 - Nikon Coolpix 4500 equipped with FC-E8 fisheye lens converter

Recently, DSLR (Digital single lens reflex) cameras have become much more affordable and their resolution has increased greatly, but thorough appraisals using DSLR cameras are still poorly documented (Pekin and Macfarlane 2009). This section solely refers to Coolpix compact camera setup; however, a comparison between compact (point and shoot) and DSLR cameras was performed in the chapter (6) of the study.

All images were collected as 'FINE' quality and at maximum resolution JPEG. Photographs were taken at a height of 1.5 m, on a grid of sample points, which were located near the littertraps. Images were collected between June and August 2011 and 2012. In each plot, 15-25 cover images (DCP) and 9-15 fisheye images (DHP) were collected, according to the stand density and structure.

Fisheye images (DHP) were collected close to sunrise (or sunset) under uniform sky conditions. The Coolpix 4500 was equipped with a FC-E8 fisheye lens converter, and was set to F1; the lens was aligned to magnetic north and pointed upward using a self-levelling tripod. The aperture was set to the minimum (F 5.3) and with the camera in aperture-priority (A) mode; the exposure was metered in an adjacent clearing. Subsequently, the mode was changed to manual (M) and the shutter speed was lowered by two stops in comparison to the exposure metered in the clearing. To investigate the influence of camera exposure on the accuracy of gap fraction from DHP, different exposure were also collected, by setting an exposure bracketing, respectively of

+1,+2,+3,+4 stops, relative to the open sky reference measured in an adjacent clearing (0). 57.5 degree images were derived from fisheye images.

Unlike fisheye imagery, DCP uses a narrow field of view (about 30°); the method does not require a fisheye converter and exposure is automatically set. Cover images were collected during the morning under uniform sky conditions. The camera was set to F2, aperture-priority mode (A) and minimum aperture (F 9.6). The fixed lens was pointed upward using a self-levelling tripod.

Cover images were then analyzed in colour using the freeware GIMP 2.6 (GNU image manipulation program; www.gimp.org). Large gaps (g_L) between tree crowns were selected using the 'fuzzy' tool, and the total number of relative pixels was recorded from the histogram. All gaps were then selected using the 'select by color' tool, and the relative number of pixels within each gap (g_T) was recorded from the histogram.

3.2.4 Comparison of LAI 2000 PCA and AccuPAR ceptometer

The LAI-2000 PCA measurements were performed in each plot between June and August 2011 and 2012, just after dawn or close to sunset, under uniform sky conditions. One above-canopy reference measurement for each plot was recorded in clearings near each study area. The fisheye lens of the instrument was covered by a 90° view cap to avoid the influence of surrounding trees on the reference measurements (Cutini et al. 1998). Nine to 15 below-canopy measurements were recorded within each plot at the same grid points used for photography. From the raw data recorded by the instrument, LAI was calculated with (LAI C) and without (LAI NC) correction for clumping (see section 5 for major details). An apparent clumping index (Ω_{APP}) was calculated as the ratio of LAI NC to LAI C, even though clumping is considered above the shoot scale (between-crowns).

LAI was also estimated from transmitted light values measured with AccuPAR ceptometers, making use of the Beer-Lambert's law (Bolstad and Gower, 1990; Cutini, 1996; Pierce and Running, 1988). This procedure needs a light extinction coefficient (k), which in this study was assumed to be $k = 0.50$ (spherical distribution), because of the difficulty of directly measuring k.

4. Estimation of canopy properties in deciduous forests with digital photography

4.1 Methods

4.1.1 Software image analysis

The gamma function of all fisheye and 57.5 degree images was corrected to 1.0 using Irfanview 3.95 before conducting hemispherical software image analysis. To assess the effect of the camera's gamma function on gap fraction and LAI retrieval, non-corrected hemispherical and 57.5 degree images (gamma= 2.2) were also processed. Fisheye (DHP) and 57.5 degree images were then analyzed using Winscanopy 2012a (Regent Instruments, Ste-Foy, Quebec, Canada). The blue channel of each image was used for processing. This is manly desirable because in the blue band of the electromagnetic spectrum, the foliage appears darker than in the other bands, thus minimizing the interference of multiple scattering in the canopy and chromatic aberration (Zhang et al. 2005). In addition, in diffuse sky conditions –namely the sky condition being considered in DHP - sky is saturated in the blue band, and thus appears white in 8-bit blue channel (Leblanc 2008), thereby improving thresholding procedures.

Fisheye images were also sharpened (medium), to enhance the contrast between sky and non sky elements. The hemisphere of each image was divided into 7 zenith angle rings and 8 azimuth segments. The zenithal angle range used for the analyses was 0-70°.

Among the outputs, canopy openness, LAI, mean leaf inclination angle and foliage clumping were derived. LAI without correction for clumping (LAI NC) was calculated by averaging the generalized LAI-2000 method (Welles and Norman 1991) and the ellipsoidal LAI method (Campbell 1986), for unmodified gap fraction data for each image (non segmented method). The ellipsoidal LAI method (Campbell 1986) was also used to calculate the mean leaf inclination angle.

LAI corrected for clumping was calculated in three different ways: first, LAI was corrected using the Lang and Xiang (1986) method, obtained by averaging the generalized LAI-2000 method and the ellipsoidal LAI method, considering the logarithm of gap fraction calculated for each azimuth segment, and the resulting log transformed gap fraction data for each image (segmented method; Lang and Xiang 1986). Further details on how gap fraction and clumping were computed using both non segmented and segmented methods were provided in chapter 5.The gap fraction distribution was also corrected for foliage clumping using the gap size distribution method (Chen and Cihlar 1995; Leblanc 2002) or by combining the gap fraction distribution and the gap size

distribution approaches (Leblanc 2005). Based on previous visual inspections, gaps larger than 500 pixels were classified as large gaps and not included in the calculation of crown porosity from DHP (the within-crown gap fraction to which Beer-Lambert's law is applied). The Lang and Xiang (1986) correction was abbreviated as LX, the Chen and Cihlar method (1995) as CC and the combined method (Leblanc et al. 2005) as CLX.

Estimates of woody materials were obtained by collecting and analyzing fisheye images during leafless; results indicated that woody area index averaged 0.71 ± 0.05 in beech, averaged 0.39 ± 0.01 in Turkey oak, averaged 0.38 ± 0.01 in chestnut. However, woody materials were not included in statistical analysis, assuming that leaves tend to present themselves to obscure underlying stems from sun (Kucharik et al. 1998). In doing so, LAI estimates from digital photography are equivalent to Plant Area Index (Bréda 2003).

The percent fraction of direct, relative and total transmittance (respectively the direct, indirect, and total site factor outputs, multiplied by 100) was also estimated from DHP, under the assumption of a standard overcast sky model (Anderson, 1966).

The blue channel of fisheye images was also analyzed with the freeware Gap Light Analyzer 2.0 (GLA; Frazer et al. 1999). Since pixel classification between sky and canopy (thresholding) in GLA was performed manually, while it is automatically determined in Winscanopy, the latter automatic threshold for both software analyses was used, to avoid subjectivity (Jarčuška et al. 2010). LAI (NC) was considered to be the LAI 5 ring output result. Also, the percent transmittance (% transmittance direct, diffuse and total outputs) was estimated, under the assumption of a standard overcast sky model.

57.5 degree photography was derived from fisheye photography using Winscanopy software. From 57.5° view angle, LAI NC and LAI LX was assumed to be LAI derived using unmodified gap fraction data (non segmented method) and log-transformed gap fraction data (segmented method), respectively. LAI CC and LAI CLX were also derived from 57.5 degree photography. For simplicity, even in this case the contribution of woody elements in leaf area calculations was neglected. Anyway, WAI estimates obtained during leafless indicates the large contribution of woody elements at 57.5 zenith angle: woody area index averaged 2.03 ± 0.55 in beech, averaged 0.70 ± 0.06 in Turkey oak, and averaged 1.27 ± 0.06 in chestnut.

Cover images (DCP) were analyzed in colour using the freeware GIMP 2.6 (GNU image manipulation program; www.gimp.org). The number of pixels contained in large gaps as well as in total gaps was used to estimate crown cover (*fc*, equation 8), foliage cover (*ff*, equation 9), porosity (φ, equation 10) as described by Macfarlane et al. (2007c):

$$f_c = 1 - \frac{g_L}{2272x1704} \tag{8}$$

$$f_f = 1 - \frac{g_T}{2272x1704} \tag{9}$$

$$\phi = 1 - \frac{f_f}{f_c} \tag{10}$$

Since, the gap removal procedure was also automated in Winscanopy (since 2006a version), another objective was to compare the performance of manual and automated classification procedures. Among the outputs, the method provided LAI, with either Chen and Cihlar (1995) correction for clumping (LAI CC, equation 11) or without correction (LAI NC, equation 12) and making use of a modified Beer-Lambert law:

$$LAI \cdot CC = -f_c \frac{\ln(\phi)}{k} \tag{11}$$

$$LAI \cdot NC = -\frac{\ln(1 - f_f)}{k} \tag{12}$$

The contribution of woody elements was assumed not significant at the narrow and vertical zenith angle used in DCP. The clumping index at the zenith was calculated as (Ω_0, Equation 13):

$$\Omega_0 = \frac{(1-\phi)\ln(1-f_f)}{\ln(\phi) f_f} \tag{13}$$

However, DCP needs a zenithal light extinction coefficient (k) to calculate LAI. Measures of zenithal extinction coefficients are challenging to obtain (Ryu et al. 2010b); also, k for DCP has been accurately evaluated only for Eucalyptus *spp.* (Macfarlane et al. 2007a, 2007b). Because measuring k is difficult, a spherical leaf angle distribution was first assumed (zenithal extinction coefficient of 0.50). However, a calculated k was obtained by combining direct measurements of LAI by the litterfall method (LAI_{LT}) with measurements of crown cover and porosity from DCP (Equation 14), to verify the spherical distribution assumption:

$$k = -\frac{f_c \ln(\phi)}{LAI_{LT}} \quad (14)$$

4.1.2 Statistical analyses

The output results from both fisheye and non-fisheye imagery were first compared with the reference methods, to evaluate the accuracy of the digital photography methods. LAI_{LT} was compared with digital photography output results by analyzing the root mean-squared error (RMSE). Methods with a small RMSE were then compared using reduced major axis (RMA) regression because the assumption that measurement errors were similar in both the direct and indirect methods (Warton et al. 2006). The RMSE of the other indirect methods commonly used for estimating LAI (LAI-2000 PCA and canopy transmittance methods) was also analyzed, to evaluate the performance of the different methods in relation to digital photography. Also, the transmittance estimated with the AccuPAR ceptometer with DHP output results were compared by fitting RMA regression lines.

All statistical analyses were performed using R version 2.13.1 (R Development Core Team, 2011), with the lmodel2 package uploaded.

4.2 Results

The studied stands were characterized by dense canopy cover with different attributes, as a consequence of the different silvicultural treatment applied (Table 2). Leaf litter ranged from 2.910 to 4.200 Mg ha^{-1} in beech, from 2.091 to 4.030 Mg ha^{-1} in Turkey oak, and from 2.865 to 3.555 Mg ha^{-1} in chestnut. LAI_{LT} ranged from to 2.6 to 8.1, with a coefficient of variation of 29.3 %. More specifically, LAI_{LT} averaged 6.9 ± 0.5 m^2 m^{-2} in beech, averaged 4.0 ± 0.4 m^2 m^{-2} in Turkey oak, and averaged 5.0 ± 0.2 m^2 m^{-2} in chestnut. Transmittance values ranged from 0.3% to 18.5% when measured in sunny conditions, while they ranged from 0.7% to 29.4% when measured in overcast sky conditions, with a coefficient of variation of 71.2% and 69.4 %, respectively.

The gap fraction obtained from fisheye images, cover images and LAI-2000 PCA were similar, although cover photography provided slightly larger gap fraction at the zenith (Figure 8). Gap fraction obtained from AccuPAR in diffuse sky conditions was similar to that obtained with DCP. By contrast, gap fraction measured with AccuPAR in sunny conditions was noticeably lower than those obtained with the other methods (Figure 8).

Table 2 Main stand characteristics of the studied stands

Species	2011 Leaf litter (Mg ha^{-1})	2012 Leaf litter (Mg ha^{-1})	2011 SLA (cm^2 g^{-1})	2012 SLA (cm^2 g^{-1})	2011 LAI_{LT} (m^2 m^{-2})	2012 LAI_{LT} (m^2 m^{-2})	2011 Transmittance* (%)	2012 Transmittance* (%)
Turkey oak	3,604	2,175	140,40	125,54	4,44	2,94	6,20	18,47
Turkey oak	3,312	2,091	146,81	109,34	3,91	2,62	8,21	16,65
Turkey oak	3,968	2,581	160,73	134,39	4,78	3,99	8,05	18,21
Turkey oak	4,030	3,232	167,32	136,11	4,44	4,89	7,34	14,62
beech	2,910	3,114	160,73	157,09	5,16	5,45	11,56	3,72
beech	3,941	4,200	167,32	167,71	7,34	7,52	1,63	0,56
beech	3,854	3,627	169,81	195,32	7,14	8,09	4,26	0,34
beech	3,259	4,062	190,76	182,50	6,66	7,92	3,14	0,61
chestnut	3,236	3,555	140,40	146,00	4,83	5,52	8,92	11,78
chestnut	2,856	3,098	146,81	146,54	4,46	4,83	6,72	6,88
chestnut	-	3,163	-	156,29	-	5,26	-	7,11

* transmittance values refer to those measured in sunny conditions.

Photographic exposure influences the magnitude of gap fraction in DHP (Figure 9). Gap fraction increased as camera exposure increased; conversely, LAI decreased with the increase in exposure. As the relative exposure increases from 0 (open sky reference) to +1, +2, +3, +4, the gap fraction increases by 186, 313, 488 and 772%, respectively.

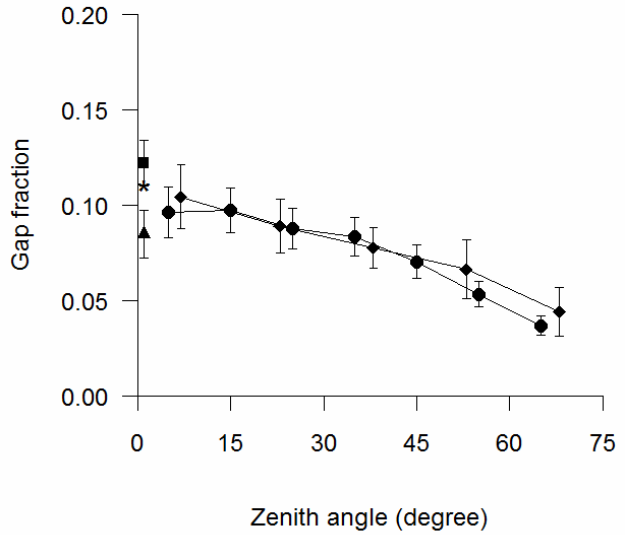

Figure 8 - Gap fraction vs zenith angle calculated from DHP (circles) and PCA (diamonds). Gap fraction near the zenith are also showed for DCP (square) and AccuPAR, either measured in sunny conditions (triangle) or in overcast sky conditions (asterisk). Standard errors are reported. To improve readability, the standard errors are not showed for AccuPAR measured in overcast sky conditions.

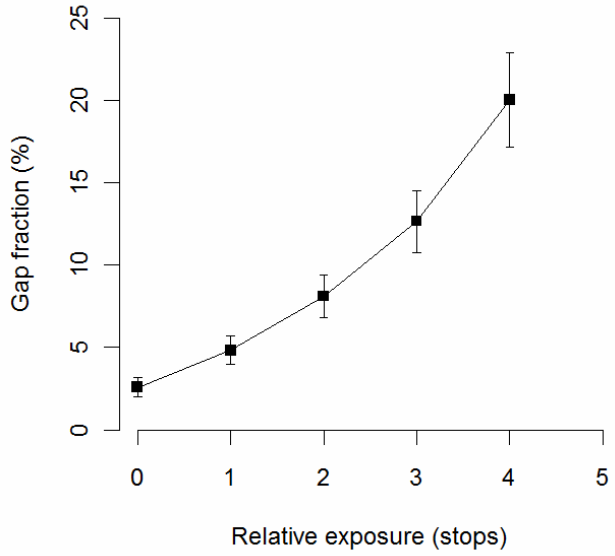

Figure 9 - Variation of gap fraction with camera exposure in DHP. The relative exposure 0 refers to the sky reference.

From DCP, crown cover, foliage cover and crown porosity ranged from 0.86 to 0.99 (average 0.93 ± 0.01), 0.78 to 0.96 (average 0.88 ± 0.01) and 0.03 to 0.13 (average 0.06 ± 0.005), respectively. Cover increased as LAI_{LT} increased, while crown porosity decreased (Figure 10). Compared on a sub-sample of cover images, a good agreement was found between crown cover estimates using either automatic or manual classification ($f_{cAUTOMATIC}$ = 0.89 $f_{cMANUAL}$+0.11, R^2=0.99, n= 52, p<0.05). By contrast, manual classification provided significantly lower estimates of crown porosity, as compared with automated procedure ($\Phi_{AUTOMATIC}$ = 0.26 Φ_{MANUAL} + 0.01, R^2=0.53, n=52, p=0.16), even though the difference did not significantly affect Ω_0 nor LAI estimated from the two procedures (data not shown).

The zenithal clumping index from DCP (Ω_0) averaged 0.81 ± 0.02; Ω_{LX}, Ω_{CC} and Ω_{CLX} from DHP averaged 0.86 ± 0.01, 0.93 ± 0.01 and 0.80 ± 0.02, respectively. Ω_{LX}, Ω_{CC} and Ω_{CLX} from 57.5 averaged 0.82 ± 0.01, 0.93 ± 0.01 and 0.76 ± 0.02, respectively. All the clumping indexes increased with increasing LAI_{LT} (Figure 10 and Figure 11); moreover, all the clumping indexes were significantly correlated (Pearson's r, $p < 0.05$). The apparent clumping index from PCA averaged 0.94 ± 0.01, which indicated little between-crowns clumping effect.

The zenithal extinction coefficient calculated from DCP and LAI_{LT} (Equation 14) averaged 0.53 ± 0.03 and agreed closely to a spherical distribution assumption (k_0 = 0.50). However, the k values appeared sensitive to canopy density and decreased as LAI_{LT} increased (Figure 10). Moreover, there was significant effect of species on calculated k (ANCOVA, $p < 0.001$). The zenithal extinction coefficient for Turkey oak, beech and chestnut averaged 0.63 ± 0.01, 0.48 ± 0.03 and 0.49 ± 0.03, respectively.

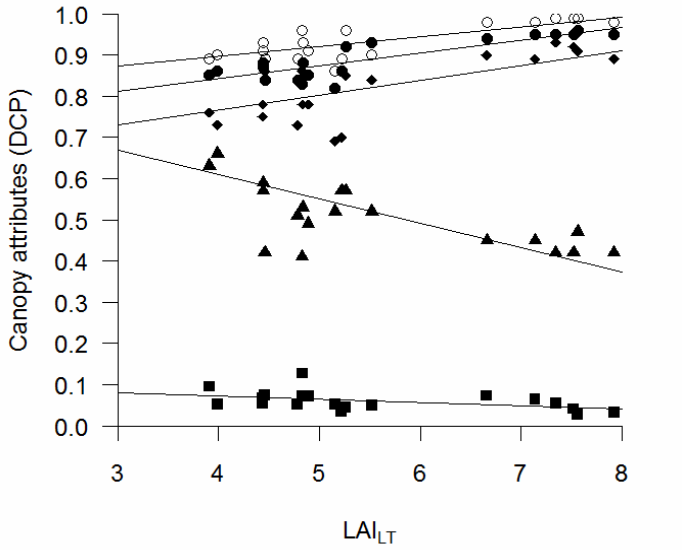

Figure 10 - Foliage cover (filled circles), crown cover (empty circles), crown porosity (squares), zenithal extinction coefficient (triangles), zenithal clumping index (diamonds) from DCP vs LAI_{LT} from the litterfall method.

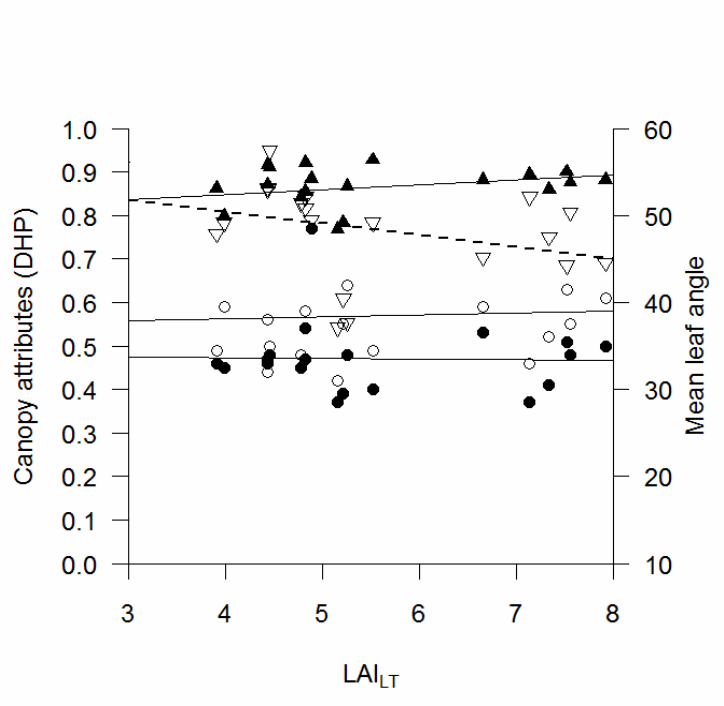

Figure 11 Foliage projection coefficient, averaged for all zenith angles (filled circles), zenithal extinction coefficient (empty circles), Ω_{LX} (filled triangles), mean leaf angle (open triangles) from DHP *vs* LAI_{LT}. To improve readability, only the outputs calculated after correction for clumping and only the LX clumping index were drawn; also, the dashed lines indicated the mean leaf angle trend.

The foliage projection coefficient (G(θ)) calculated from DHP even showed an approximately spherical leaf angle distribution, at least for zenith angle up to 30°, in particular when correction for clumping (LX) was applied (Figure 12). Both G(θ) (averaged for all zenith angles) and mean leaf angle decreased as LAI_{LT} increased, but *k* near the zenith increased (Figure 11). The G(57.5) showed a more vertical leaf angle compared to the spherical assumption made in 57.5 photography, in particular when correction for clumping was applied ($G_{57.5}$~0.40). There was no effect of species on both G(θ) and *k* from DHP (ANCOVA).

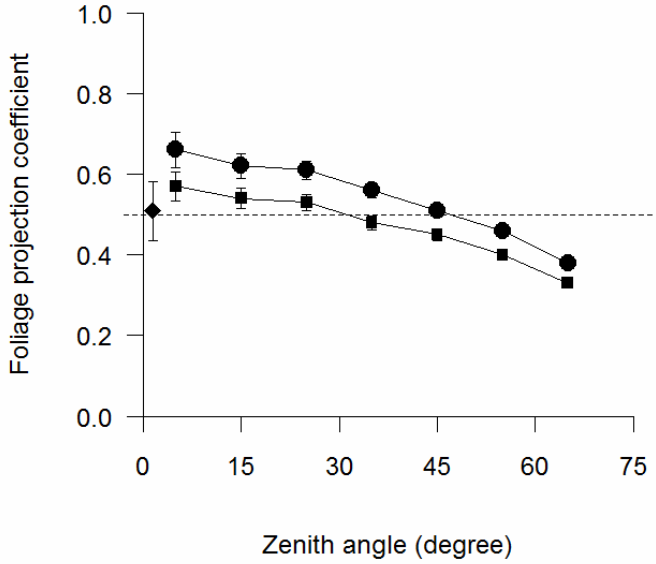

Figure 12 - Foliage projection coefficient *vs* zenith angle before (circles) and after (squares) LX correction for clumping from DHP. The dashed line represents the spherical leaf angle distribution. Foliage projection coefficient near the zenith is also presented from DCP (diamond). Standard errors are reported.

With regard to LAI, similar RMSE were obtained from fisheye images using Winscanopy, regardless of whether the images were gamma corrected or not, and regardless of which clumping correction (if any) was applied (Table 3). Similar RMSE values were also obtained from DCP, regardless of whether clumping correction was applied. Small RMSE values were obtained from 57.5 degree images without gamma correction. Overall, the CLX correction for clumping produced poorer results than the other two clumping indexes. Poor results were also obtained from fisheye images using GLA software and using LAI-2000 PCA. Worse results were obtained with canopy transmittance method (Table 3).

Methods in which the RMSE was equal or below to 0.6 were further analyzed using RMA regression (Table 4). On the basis of the RMA regression results, the DHP method outperformed the DCP method, because the slopes were closer to unity and the intercepts were closer to zero than for the DCP method (Table 4), even though both methods showed high correlation with LAI_{LT}

values. The DHP method also outperformed the 57.5 degree method, because the slopes were closer to unity and the intercepts were closer to zero than 57.5 degree method. The best results from DHP were obtained when the images were gamma corrected; the LX clumping correction performed best, followed by no clumping correction at all. The best results from 57.5 degree were obtained when the images were gamma corrected, and when no clumping correction was applied.

Table 3 - RMSE of LAI values from indirect methods and from LAI_{LT} from littertraps.

Method	Gamma	NC	LX	CC	CLX
Digital Cover Photography	2.2	0.44	-	0.45	-
Digital Hemispherical Photography - GLA	1.0	0.73	-	-	-
Digital Hemispherical Photography - GLA	2.2	0.73	-	-	-
Digital Hemispherical Photography - Winscanopy	1.0	0.49	0.52	0.44	0.57
Digital Hemispherical Photography - Winscanopy	2.2	0.33	0.37	0.56	0.60
57.5 Degree - Winscanopy	1.0	0.57	0.59	0.60	0.72
57.5 Degree - Winscanopy	2.2	0.46	0.37	0.46	0.65
PCA-LAI 2000	-	0.65	0.62	-	-
Canopy Transmittance method - OVERCAST	-	1.48	-	-	-
Canopy Transmittance method - SUNNY	-	1.52	-	-	-

Table 4 - RMA regression coeffeicients for LAI from indirect methods and from LAI_{LT} from littertraps. The expression used for regression was: $LAI_{indirect} = a\ LAI_{LT} + b$

Method	Correction	Gamma	*a*	*b*	R^2	*p*
DCP	NC	2,2	0,66	1,14	0,82	0,01
	CC	2,2	0,52	2,90	0,73	0,01
DHP-Winscanopy	NC	1,0	0,72	**0,18**	0,79	0,01
	LX	1,0	**0,77**	**0,49**	0,78	0,01
	CC	1,0	0,52	1,36	0,74	0,01
	CLX	1,0	0,55	1,87	0,63	0,01
	NC	2,2	0,50	**0,58**	0,83	0,01
	LX	2,2	0,55	0,75	0,82	0,01
	CC	2,2	0,36	2,02	0,57	0,01
	CLX	2,2	0,41	2,28	0,54	0,01
57.5 degree	NC	1,0	0,56	**1,22**	0,63	0,01
	LX	1,0	0,52	2,65	0,59	0,01
	CC	1,0	0,56	**0,94**	0,59	0,01
	NC	2,2	0,45	1,12	0,63	0,01
	LX	2,2	0,50	1,85	0,63	0,01
	CC	2,2	0,35	1,97	0,51	0,01

Highlighted in bold are intercepts for which the 95 % confidence interval includes zero, and slopes that do not significantly differ from one ($p < 0.05$).

On average, DHP underestimated LAI (Figure 13) when compared with LAI_{LT} values, with an average underestimation of -24.9%. Underestimation was lower when correction for clumping was applied in DHP, arriving at -13.3%, -22.2% and -9.9% when LX, CC and CLX clumping correction was applied, respectively. The accuracy of LAI estimates from DHP appeared insensitive to LAI_{LT} values, unlike the other two photographic methods (Figure 13). Prior to correcting for

clumping, DCP generally underestimated LAI, with an average underestimation of -12.5%. After correcting for clumping, DCP overestimated LAI in the less dense canopies ($LAI_{LT} < 5.5$) while underestimated LAI in the more dense canopies ($LAI_{LT} > 5.5$). A similar pattern was also observed in 57.5 degree photography (Figure 13).

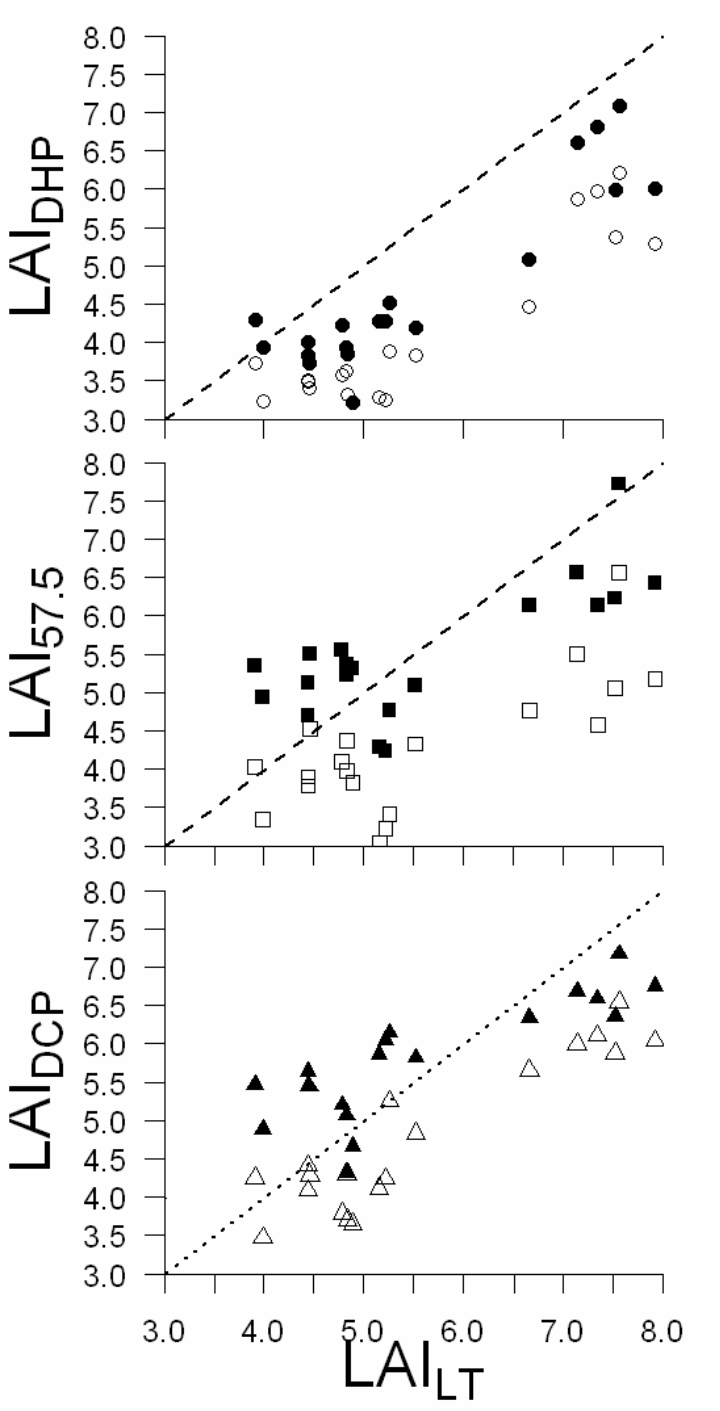

Figure 13 – Leaf area index from digital photography *vs* LAI_{LT} from litterfall method. For DHP, data are presented, either with LX correction for clumping (filled circles) or without correction for clumping (empty circles). For 57.5, data are presented, either with LX correction for clumping (filled squares) or without correction for clumping (empty squares). For DCP, data are presented, either with CC correction for clumping (filled triangles) or without correction for clumping (empty triangles). The dashed lines indicate the 1:1 relationships.

Foliage cover and crown cover were strongly correlated with LAI from DHP; 95% confidence intervals for all the intercepts did not include zero:

$f_f = 0.71 + 0.044$ LAI NC, $p = 0.01$, $R^2 = 0.75$ (15)

$f_f = 0.70 + 0.039$ LAI LX, $p = 0.01$, $R^2 = 0.71$ (16)

$f_c = 0.79 + 0.035$ LAI NC, $p = 0.01$, $R^2 = 0.71$ (17)

$f_c = 0.79 + 0.031$ LAI LX, $p = 0.01$, $R^2 = 0.64$ (18)

With regard to transmittance, a strong correlation was found between values estimated from DHP and from AccuPAR ceptometer obtained under either sunny or overcast sky conditions (Table 5). Better fit between the two methods was obtained when reference measurements were made in sunny conditions. The Winscanopy software outperformed the GLA software, because of the higher correlation with AccuPAR measures, slopes closer to unity and intercepts closer to zero than those obtained using GLA. However, the high RMSE obtained (~1.5) suggested the results should be interpreted with caution. The high variability observed in transmittance values measured with ceptometer (CV~70%) probably affected the accuracy of reference measurements; as such, results should be treated with caution.

Table 5 – RMA regression coefficients from fisheye photography and AccuPAR ceptometer. The expression for regression was: $y_{DHP} = a\ x_{AccuPAR} + b$.

Software	Reference sky	y	*a*	*b*	R^2	*p*
GLA	Sunny	DIF	**0.67**	**0.86**	0.46	0.01
	Sunny	DIR	**0.73**	**0.51**	0.40	0.01
	Sunny	TOT	**0.65**	**1.15**	0.46	0.01
WINSCANOPY	Sunny	DIF	**0.71**	**1.35**	0.50	0.01
	Sunny	DIR	**0.87**	**0.73**	0.62	0.01
	Sunny	TOT	**0.79**	**1.44**	0.62	0.01
GLA	Overcast	DIF	**0.52**	**-0.74**	0.41	0.04
	Overcast	DIR	0.44	0.39	0.16	0.15
	Overcast	TOT	**0.44**	**0.29**	0.30	0.05
WINSCANOPY	Overcast	DIF	**0.49**	**0.40**	0.34	0.02
	Overcast	DIR	**0.62**	**0.01**	0.45	0.02
	Overcast	TOT	**0.60**	**0.09**	0.44	0.03

Highlighted in bold are intercepts for which the 95 % confidence interval includes zero, and slopes that do not significantly differ from one ($p < 0.05$). DIF, DIR and TOT refer to diffuse, direct and total percent transmitted radiation, respectively.

There was good agreement between the two software packages used to process DHP (GLA and -Winscanopy; Table 6). A strong correlation between the two software outputs was found in all the variables tested, and all the regressions were significant. Overall, the RMA regression analysis showed the tendency of GLA to underestimate the variables, compared with Winscanopy; thus, Winscanopy outperformed GLA software.

Table 6 – RMA regression coefficients obtained from fisheye photography using GLA and Winscanopy software package. The expressions for regressions were: $y_{GLA} = a\ X_{WINSCANOPY} + b$.

y	*a*	*b*	R^2	*p*
LAI NC	**0.85**	**0.27**	0.48	0.01
Openness	0.76	**-0.38**	0.91	0.01
DIF	**0.93**	**-0.27**	0.87	0.01
DIR	**0.86**	**-0.26**	0.75	0.01
TOT	**0.83**	**-0.09**	0.86	0.01

Highlighted in bold are intercepts for which the 95 % confidence interval includes zero, and slopes that do not significantly differ from one ($p < 0.05$). DIF, DIR and TOT refer to diffuse, direct and total percent transmitted radiation, respectively.

4.3 Discussion

Although data were collected from stands with different species composition, ages, structures and silvicultural treatments, LAI estimated by litter traps was in the range of values reported for deciduous forests (Jarvis and Leverenz 1983). In particular, previous studies reported LAI values estimated by litter traps for beech forests ranging from 5.0 to 10.2 (Bréda 2003; Lebourgeois et al. 2005; Meier and Leuschner 2008) and LAI values for deciduous forests of chestnut and oak spp. Ranging from 1.71 to 7.45 (Dufrêne and Bréda 1995; Thimonier et al. 2010).

Despite the great differences in the plot area sampled between litterfall and indirect methods, estimates of LAI from digital photographic methods that agreed with LAI from litter traps to within ± 25 % were obtained; hence, LAI_{LT} can represent the largest effective plot area sampled in DHP.

Dense and overstocked forest stands usually represent challenges to the accurate estimation of canopy properties. In the present study, all digital photographic methods provided estimates of canopy properties that satisfactorily agreed with the reference methods, in spite of the differences in theoretical background, field procedures and processing steps.

With respect to LAI, fisheye photography showed a tendency to underestimate LAI compared with the litter traps method. Average underestimation decreased when correction for clumping was applied, which agrees with results from other studies (Chen and Cihlar 1995; Lang and Xiang 1986; Leblanc 2002; Macfarlane et al 2007b; Van Gardingen et al. 1999). This result is probably caused by the tendency of foliage to concentrate in the upper part of the crown, which is frequent in stand with dense canopy cover, thus resulting in a non-random distribution of foliage

within the canopy (Sampson and Allen 1995). This was also supported by the clumping indices calculated from both DHP and DCP, which invalidates the random distribution assumption. Moreover, the clumping indices appeared to decrease as LAI_{LT} increased, where presumably the degree of clumping that can be detected was less (Van Gardingen et al. 1999). Conversely, the apparent clumping index from PCA showed $\Omega_{APP} \sim 0.94$, which would indicate little-between crowns clumping. As such, dense canopies were characterized by higher within-crown than between-crowns clumping. It is reasonable to infer that the more azimuth segments were used, the more heterogeneity is detected (Van Gardingen et al. 1999). This also implies that small segments can detect clumping better than large segments; it is likely that use of a single (wide) azimuth segment was unable to yield a reliable and useful clumping index in dense canopies; this method, however, might be more applicable in sparse and heterogeneous canopies, in which clumping occurs greatly at stand scale.

Gap fraction estimated at the zenith from DCP was quite larger than those from DHP, probably because DCP had higher vertical resolution, which may result in better accuracy in detecting small gaps in dense canopies, as compared to DHP. Previous studies reported the accuracy of DCP in assessing gap fraction in sparse to moderately dense canopies (Macfarlane et al. 2007b; Pekin and Macfarlane 2009; Ryu et al. 2010b). The current study even supported the accuracy of DCP in assessing gap fraction in more dense canopies.

Since gap fraction from DCP was correctly estimated, and since the clumping correction used in DCP can be considered accurate, it was possible to derive reliable *k* values to verify the spherical leaf angle assumption. On average, the calculated *k* suggested a nearly spherical leaf angle distribution; nonetheless, an apparent sensitivity of *k* to LAI was observed in this study, which was in accordance with previous reports (Cannell et al. 1987; Johansson 1989; Macfarlane et al. 2007a; Smith et al. 1991). However, different *k* values would probably reflect species differences, rather than LAI differences, as observed in the current analysis. As such, the different *k* values obtained for the three species can be regarded as reliable, and can be further applied for routine LAI estimation in deciduous stands. Nonetheless, Bolstad and Gower (1990) found error in LAI estimation was 6% when *k* was measured, but increased to 20% when *k* was assumed. This implies that direct measurement of *k* is preferable, whereas it was possible.

Similar considerations can be made regarding the spherical leaf angle assumption implied in 57.5 degree photography, on account of the similar pattern observed in LAI estimates between 57.5 and DCP. Moreover, the calculated G from 57.5 showed a more vertical leaf angle (G~0.4) than the spherical leaf angle distribution, in particular when correction for clumping was applied. The lower performance in 57.5, when compared with DCP, could also result from the lower resolution and smaller area sampled in 57.5; hence, the number of 57.5 images collected may have been

insufficient to accurately estimate small gap within dense canopies. Although not included in the analysis, the large contribution of woody to leaf area at 57.5° is a major drawback, which should be taken into duly account as a possible source of uncertainty related to 57.5° photography.

In contrast to the DCP and 57.5 methods, the frequency of LAI underestimation was relatively constant with corrected DHP, because the extinction coefficient is not assumed but automatically estimated. DHP also suggested a nearly spherical leaf angle distribution, although foliage angle distribution function calculated from fisheye images should be treated with caution (Macfarlane et al. 2007a). The zenithal extinction coefficient calculated from fisheye image appeared to increase as LAI increased, while the mean leaf angle decreased, thus showing an opposite trend comparing with DCP. Similar results were also observed by Macfarlane et al. (2007a). Accordingly, poor sampling near the zenith from hemispherical sensor limits the accuracy of *k* near the zenith from DHP (Macfarlane et al. 2007c).

An inherent limitation of hemispherical photography is the need to set an adequate exposure manually, which dramatically affects LAI estimation, especially in dense canopies (Chen et al. 1991; Zhang et al. 2005). In the present study, adjustment by two stops of overexposure relative to the open sky reference was used, based on previous reports (Macfarlane et al. 2007c; Zhang et al. 2005), and was supported by the accurate gap fraction obtained from DHP. In addition, good results from DHP (and 57.5) were obtained when images were gamma corrected; gamma correction therefore represents an additional step in the DHP image-processing procedure, which was already more tedious and time-consuming (Jonckheere et al. 2004; Macfarlane et al. 2007c) compared with DCP.

One advantage of DHP is the ability to estimate parameters related to the forest light environment. In the present study good estimates of transmittance were obtained, which agreed with those recorded with an AccuPAR ceptometer. All of the radiation parameters were correlated with the reference method. However, the high RMSE suggested these results must be treated with caution. It is likely that the number of reference sample points collected should be larger than that used in the current study.

The two software packages used in DHP analysis showed marked differences in performance. Overall, Winscanopy performed better than GLA. One advantage of the former is that pixel classification in the canopy and sky (thresholding) is performed automatically, whereas in GLA it is performed manually; thus, greater human input is required with GLA, which may lead to inadequate image registration (Jarčuška et al. 2010), thereby reducing the accuracy of the estimates. In the current study the automatic Winscanopy threshold was used for both software analyses. This might have resulted in poorer estimates of LAI using GLA, since the two programs differ in the models used. Another advantage of Winscanopy is that the software is able to provide DCP

estimates (since the 2006a version), thus avoiding subjectivity in separating large gaps from small gaps. However, in the current study large gaps from DCP were estimated both manually or automatically using Winscanopy software and very little differences were observed between them in Ω_0 and LAI output results, in spite of some differences in crown porosity observed for individual images. One advantage of GLA is the software is available for free.

In summary, the agreement between the photographic and direct methods for estimating LAI and transmittance was satisfactory. Both the DHP and DCP methods showed good potential to replace other indirect methods, such as the LAI-2000 PCA and AccuPAR ceptometer, in broadleaf forests, which agrees with the findings of other studies (Leblanc et al. 2005; Macfarlane et al. 2007b). Nevertheless, users should consider the following advantages and disadvantages of the photographic methods.

- DHP is sensitive to photographic exposure, which is a major cause of error (Chen et al. 1991; Zhang et al. 2005). The gamma function and thresholding strongly affect the accuracy of the results (Cescatti, 2007; Jonckheere et al. 2005; Macfarlane et al. 2007b). Consequently, this method is tedious and time-consuming because several image-processing steps are required. Photographs must be taken close to sunrise (or sunset), not during common working hours. The main advantages of the method are DHP does not require assumptions to be made concerning the extinction coefficient and DHP also allows characterization of radiation regimes in forest canopies.
- DCP does not require measurement of photographic exposure; the method is quick, simple, and can be applied during normal working hours (Pekin and Macfarlane, 2009). DCP is able to provide additional information aside from LAI, such as crown cover, porosity, foliage cover and clumping index at the zenith (Macfarlane et al. 2007c). The major drawback of this method, the need to know the value of *k*, was confirmed in our study.
- 57.5 degree has the advantage that *k* is automatically estimated. The disadvantage of the method is that 57.5° images samples a very small zenith and azimuth angle, and therefore more samples are needed to prevent underestimation of LAI at small gap fractions. The larger number of images required and the potentially large contribute of woody elements are the two major obstacles to adoption of 57.5 degree method.

4.4 Conclusions

All the digital photographic methods are useful and inexpensive tools to quantify forest canopy properties. The more recently developed DCP method offers strong potential for indirect measurement and monitoring of LAI and other canopy properties in deciduous forests. Even

without measurement of the zenithal light extinction coefficient, the method provided accurate estimates of LAI in dense deciduous forests, assuming a spherical leaf angle distribution. Also, DCP is able to measure several parameters that characterize a forest canopy, such as crown cover, which do not require either conversion to LAI nor the foliage inclination angle distribution. So, cover photography represents a useful new procedure for monitoring deciduous forests because it is fast, inexpensive, and simple to use, permitting widespread use of the method. However, in situations where no direct reference measurements of *k* are available, and estimates of LAI are required, use of DHP in conjunction with DCP can provide a valuable ‘reality-check‘ to locally calibrate *k*, by means of correlations between LAI from DHP and *fc*, *ff* from DCP; cover photography could then be used more routinely to large areas, based on the cross-calibrated *k* values.

5. The influence of spatial resolution on clumping index retrieval in dense forest canopies: an assessment through multidirectional view canopy instruments.

Note: In this chapter the terminology was slightly different from that used in the previous chapter 4, to allow more comprehensive distinction between effective leaf area index and true leaf area index. Accordingly, the following terminology and abbreviations was used throughout the current chapter:

- Non segmented method, the analytical techniques which determines the gap fraction for a number of concentric zenith rings; available for LAI-2000 PCA and hemispherical photography (Figure 14);
- Segmented method, the analytical technique which determines the gap fraction for a number of segments within each zenith ring; available for hemispherical photography (Figure 14);
- Ω_{APP}, apparent clumping index calculated from non segmented method ;
- Ω_{LX} clumping index calculated from segmented method;
- LAI, true leaf area index (clumping correction considered);
- LAI_{eff}, effective leaf area index (no clumping correction);
- LAI_{APP}, leaf area index corrected for Ω_{APP};
- LAI_{LX}, leaf area index corrected for Ω_{LX};
- LAI_{LT} leaf area index derived from littertraps;
- Ω_{LT} reference clumping derived from $L_{LT;}$

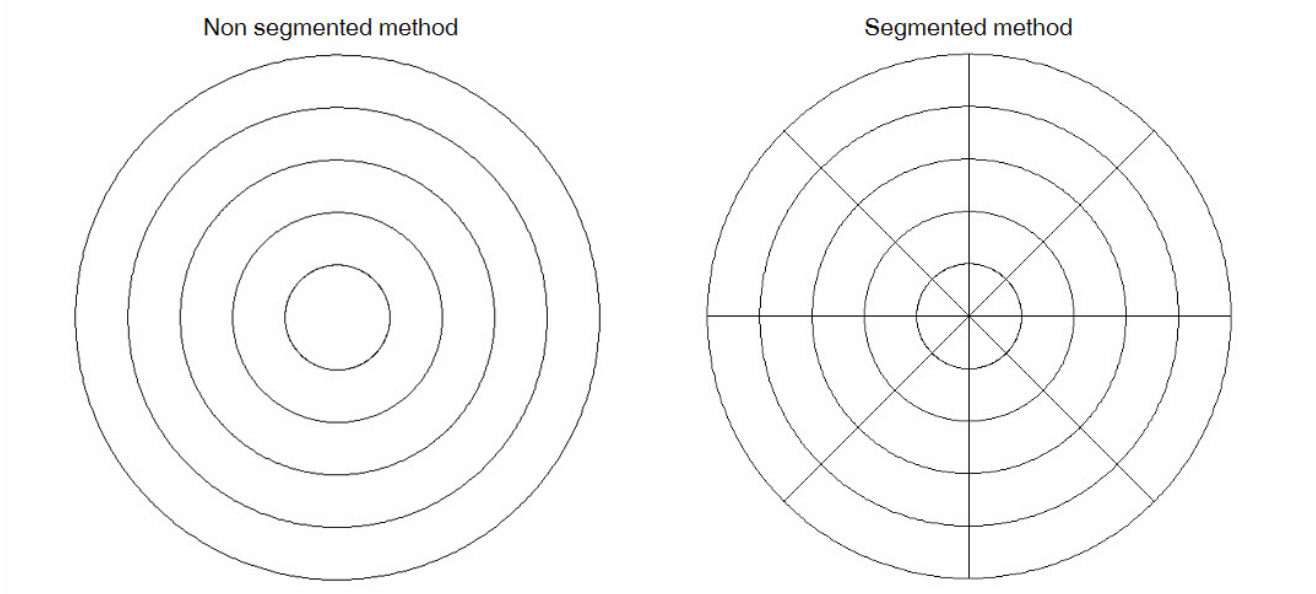

Figure 14 - Overlay of non segmented method (left) and segmented method (right) available for gap fraction analysis of fisheye images

5.1 Definitions and theory

Miller (1967) proposed a theorem for deriving LAI from Beer-Lambert's law based on multiple gap fraction measurements (Equation (19)):

$$LAI = 2\int_0^{\pi/2} -\left[\ln P(\theta)\right]\cos\theta\sin\theta d\theta \tag{19}$$

This simple approach is based on the Poisson distribution assumption that leaves are locally uniformly and randomly distributed. However, foliage non-randomness in vegetation canopies is a major challenge when deriving leaf area index through optical methods, because vegetation communities occur mainly in heterogeneous ecosystems. When gap fraction is measured in clumped canopies, indirect methods therefore estimate effective leaf area index (LAI_{eff}) rather than true leaf area index (LAI), as a results of clumping of foliage, which results in an underestimation of LAI. For this reason, the non-random distribution of foliage within the canopy should be accounted for by correcting the Beer-Lambert's law for foliage clumping (Equation (20), after Nilson et al. 1971):

$$LAI = 2\int_0^{\pi/2} -\frac{\left[\ln P(\theta)\right]}{\Omega(\theta)}\cos\theta\sin\theta d\theta \tag{20}$$

Where LAI refers to the true LAI, whereas effective LAI is defined as the product of LAI and $\Omega(\theta)$. Since leaf area index is proportional to the natural logarithm of gap fraction, Lang and Xiang (1986) stated that LAI in clumped canopies could be found more accurately by averaging the gap fraction in a logarithmic way. The approach proposed by Lang and Xiang (1986) is scale-dependent, since foliage is assumed to be randomly distributed over the length scale considered for logarithmic averaging gap fraction. It is reasonable to infer that the lower scale logarithm of gap fraction is computed, the more accurately estimates of LAI is obtained, owing to a finer scale clumping correction resulting from locally applying the Poisson distribution. This also implies that the differences between LAI_{eff} and LAI in clumped canopies would increase as the length scale at which logarithm of gap fraction is computed decrease. Hence, the performance of logarithmic averaging approach would be greatly influenced by the resolution of canopy analysis system.

If LAI is computed over multiple sample units, gap fraction can be averaged in two ways (Equation (21) and (22); Lang and Xiang 1986):

$$LAI = 2\int_0^{\pi/2} -\left[\ln \overline{P_0(\theta)}\right]\cos\theta \sin\theta d\theta \quad (21)$$

$$LAI = 2\int_0^{\pi/2} -\left[\overline{\ln P_0(\theta)}\right]\cos\theta \sin\theta d\theta \quad (22)$$

Equation (21) assumes foliage is randomly distributed within all the units as a whole, while equation (22) assumes foliage is randomly distributed within the single unit's sensor of view. For the Lang and Xiang's (1986) method, the clumping index is calculated as:

$$\Omega(\theta) = \frac{\ln\left[\overline{P(\theta)}\right]}{\overline{\ln\left[P(\theta)\right]}} \quad (23)$$

If a single unit is represented by a sample reading, equation (21) assumes foliage spatial randomness within a sample domain (e.g., a forest stand), and equation (22) would therefore potentially account for clumping effects above the sample scale (for simplicity, it was previously referred as a between-crowns clumping effects, see 2.4.2). This is the approach being used in LAI-2000 PCA (hereafter non segmented method, Figure 15); the correction for clumping would be therefore largely dependent from the sensors' field of view (azimuth range). LAI calculated from Equation 21 can be considered an effective leaf area index (LAI_{eff}), which by definition must ignore clumping (Ryu et al. 2010a). The in-built software of LAI-2000 PCA by default approximates true leaf area index using Eq. (22), which potentially account for foliage clumping effects at scales larger than the sample, (LAI_{APP}), while the more recent release of the instrument (LAI-2200 PCA) also calculates LAI_{eff} using Eq. (21). The apparent clumping index from PCA is calculated as:

$$\Omega_{APP} = \frac{LAI_{eff}}{LAI_{APP}} \quad (24)$$

The term apparent clumping index (Ω_{APP}) indicates that clumping factor is partially considered at scales larger than the sample (Ryu et al. 2010a).

On the other hand, if a sample reading is divided into a number of sub-samples (e.g., the azimuth slices within each ring), which were considered as a single independent unit, leaf area index calculated from equation (22) would account for the spatial heterogeneity within each sample reading's footprint (e.g., a fisheye image), while leaf area index calculated from equation (21) would account for clumping effects above the sample scale. This is the approach being used in DHP (segmented method, Figure 15); software image processing enables calculation of LAI corrected for

clumping effects below the sample scale (LAI_{LX}). The resulting clumping index is then calculated as:

$$\Omega_{LX} = \frac{LAI_{APP}}{LAI_{LX}} \tag{25}$$

It is worth nothing that Ω_{LX} from DHP by default incorporates the apparent clumping correction implied in PCA, due to a spatial scaling overlap between the two approaches (Figure 15). As a consequence, the Ω_{LX} might underestimate clumping effects, given that $LAI_{eff} \leq LAI_{APP} \leq LAI_{LX}$ because of the convexity of the negative logarithmic function (Jensen, 1906). A mathematical explanation is provided in annex 1.

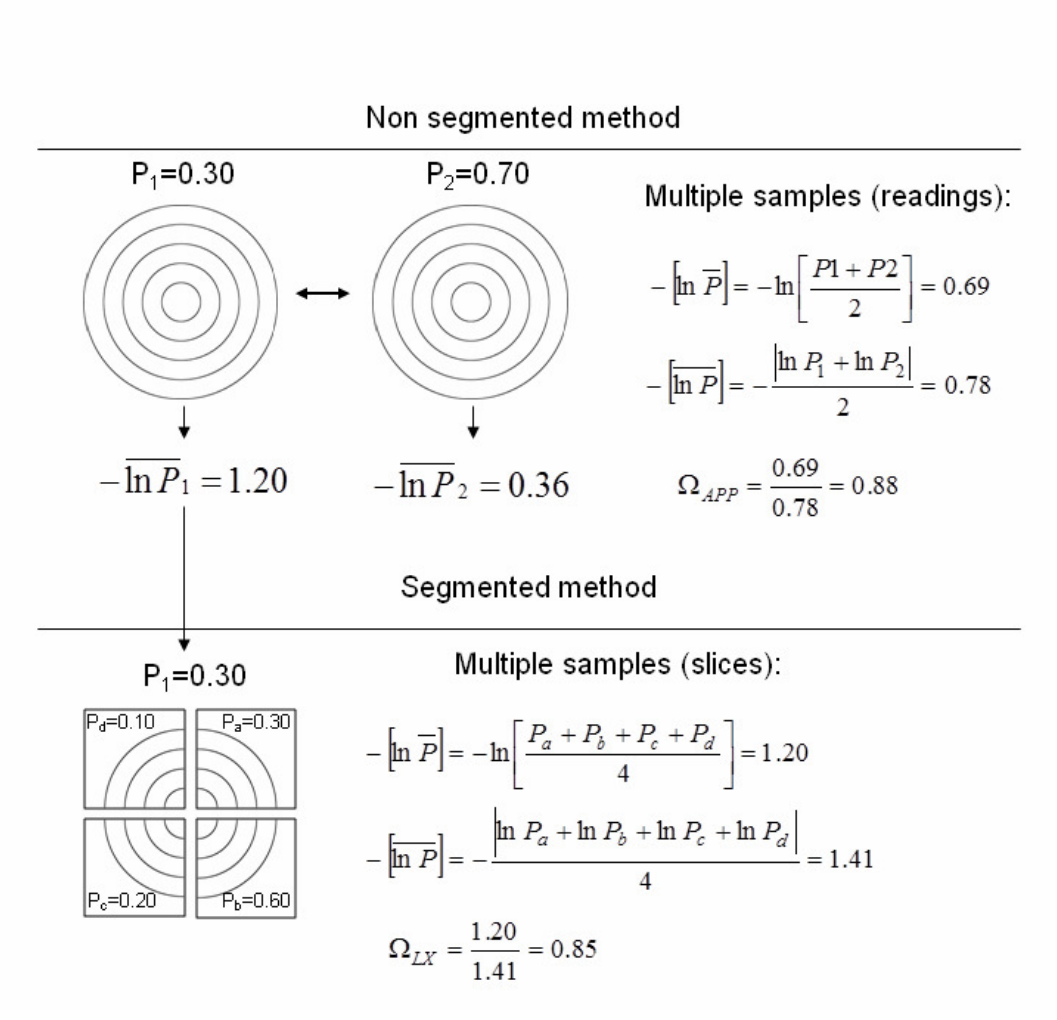

Figure 15 A conceptual diagram to calculate LAI in clumped canopies from multidirectional view canopy instruments. From non segmented method available in LAI-2000 PCA, two readings are taken. The $\ln\left[\overline{P(\theta)}\right]$ gave smaller results than that obtained from $\overline{\ln\left[P(\theta)\right]}$, implying that a Ω_{APP} clumping correction between the two measurements was applied in the latter. From segmented method available in DHP, the first reading was divided in four sub-samples which are treated as independent units. The $\ln\left[\overline{P(\theta)}\right]$ gave smaller result than that obtained from $\overline{\ln\left[P(\theta)\right]}$, implying that a Ω_{LX} clumping correction was applied in the latter. Note that the non corrected $\ln\left[\overline{P(\theta)}\right]$ calculated from segmented method

is equivalent to the corrected $\overline{\ln[P(\theta)]}$ from non segmented method, indicating that Ω_{LX} incorporates the apparent clumping correction.

In theory, increasing the number of segments – and, therefore, restricting the azimuth view within each ring's footprint – would better detect spatial heterogeneity in dense canopies, in which clumping may occur at small length-scale. However, the minimum azimuth size should also meet the Poisson theory assumption used to derive LAI from Equation (19), which assumes an infinite canopy to achieve the exponential relationship. This is motivated because segments with zero light transmission avoid LAI retrieval, since logarithm of zero is undefined. This would be a particularly relevant issue in dense canopies, in which leaves are likely to saturate the available space within a canopy.

Once $\Omega(\theta)$ is computed, the foliage projection coefficient can be more accurately estimated as:

$$G(\theta) = \frac{-\ln[P(\theta)]\cos\theta}{LAI \cdot \Omega(\theta)} \tag{26}$$

5.2 Methods

5.2.1. Software image analysis

The gamma function of all fisheye images collected by Nikon Coolpix 4500 was corrected to 1.0 using Irfanview 3.95 before conducting hemispherical software image analysis. The blue channel of the images was sharpened (medium) and then analyzed in Winscanopy 2012a (Regent Instruments, Ste-Foy, Quebec, Canada). The hemisphere of each image was divided into 5 zenith angle rings, (with central zenith angle of 7°, 21°, 36°, 51° 66°, respectively), similar to those used in LAI-2000 PCA (central zenith angle of 7°, 23°, 38° 53° 68°, respectively). Little differences between the five concentric rings used in the two devices results from noncontiguous detectors implemented by default in PCA (0-13°, 16-28°, 32-43°, 47-58°, 61-74°), whereas DHP uses contiguous rings (0-13°, 13-28°, 28-43°, 43-58°, 58-74°). However, the differences were considered negligible.

Fisheye images were first analyzed by considering all azimuth segments as a whole (non segmented method); this procedure replicates the PCA and was used to simulate PCA measurements. For each image, gap fraction was computed as the average for each ring. For multiple images (namely the images across the stand), LAI was calculated by applying two gap averaging procedures (Equation 21 and 22). LAI_{eff} and LAI_{APP} were assumed to be LAI calculated by Equation 21 and 22, respectively, with the latter approximating true LAI, a result of clumping

correction above the sample scale. An apparent clumping index (Ω_{APP}) was calculated as the ratio of LAI_{eff} to LAI_{APP}. To simulate the influence of azimuth view cap in PCA measurements, fisheye images were analyzed considering different azimuth range, comparable with those available from PCA using view caps. Specifically, the following azimuth range was analyzed: 360°, 270°, 180°, 90°, 45° and 10°. For each image, gap fraction was averaged over the selected azimuth angular widths.

On the other hand, fisheye images were further analyzed using the segmented method obtained by dividing each image into azimuth segments with 5° width over the same different azimuth range used previously: 360° (72 segments), 270° (54), 180° (36), 90° (18), 45° (9) and 10° (2). Use of minimum segment width of 5° is motivated because the minimum number required for applying the segmented analysis of gap fraction at 10° azimuth view. From segmented method, LAI_{APP} and LAI_{LX} were calculated by Eq. 21 and 22, respectively (Figure 15); the Ω_{LX} was then calculated as the ratio of LAI_{APP} to LAI_{LX}.

We judged the 5° azimuth size should be a lower limit for computing gap fraction in dense canopies, in order to avoid segments with no gap fraction (empty segments). Anyway, in situations were empty segments were still detected, the gap fraction of empty segments was recomputed using a local Poisson model (Leblanc et al. 2005):

$$P(\theta) = \exp\left(\frac{-0.5 LAI_{SAT}}{\cos\theta}\right) \tag{27}$$

Where LAI_{SAT} is maximum saturated LAI, which was set by default as 8, consistently with data calculated from littertraps. LAI and clumping indices were then calculated.

5.2.2 Comparison with LAI-2000 PCA and littertraps

The accuracy of Ω_{APP} and leaf area index estimates derived from DHP using non segmented method and 90° view cap were compared with data collected from PCA using 90° view cap. From PCA, gap fraction was calculated for each ring from the raw data collected by the instrument. LAI was then estimated for each plot by applying two different gap fraction averaging procedures (Equation 21 and 22; Ryu et al. 2010a). LAI without correction for clumping and LAI corrected for clumping was assumed to be LAI calculated by Equation 21 and 22, respectively, even though clumping effects are considered above the sample scale. An apparent clumping index was calculated as the ratio of Equation 21 to Equation 22.

In addition, foliage clumping and leaf area index derived from DHP were compared with reference values obtained from littertraps. For each azimuth range, a reference clumping index

(Ω_{LT}) was calculated by dividing LAI_{eff} derived from non segmented method by $LAI_{LT;}$ this is motivated because LAI_{eff} from non segmented method is the appropriate value for determining effective leaf area index, which by definition must ignore clumping. As a consequence, it is reasonable to consider Ω_{LT} as the best approximating true clumping index.

5.2.3 Statistical analyses

We investigate the effect of azimuth resolution in clumping index and leaf area index estimates from both non segmented and segmented methods. Two-way ANOVA analysis was used, with azimuth resolution and site treated as main effects. No interactions between site and azimuth were found; hence, the interaction term was removed from the analysis. Tukey's pair-wise comparison test was used to compare output results from different azimuth resolution range, if ANOVA indicated that a significant difference existed between them in the variable of interest. For each azimuth range, Ω_{APP} and Ω_{LX} were also compared using paired *t*–test.

The output results from DHP using both segmented and non segmented methods were compared with those derived by PCA and littertraps. Given that all methods are subject to natural variation and measurement errors and are therefore not independent variables, a Reduced Major Axis (RMA) regression was used to compare the output results from the different methods. In doing so, it is possible to verify whether the slope of the regression was one.

All statistical analyses were performed using R version 2.13.1 (R Development Core Team, 2011, with the lmodel2 package uploaded.

5.3 Results

5.3.1 The effect of azimuth resolution on clumping index and leaf area index

Based on analysis of fisheye images, different patterns were observed from either non-segmented or segmented method for clumping index estimates. Analysis revealed that Ω_{APP} significantly decreased as azimuth decrease (ANOVA, $p<0.001$; Figure 16); apparent clumping index ranged from 0.98 (360°) to 0.85 (10°). Compared with the whole 360° azimuth range, Ω_{APP} decreased by 0.8%, 1.9%, 4.5% ($p<0.001$), 7.0% ($p<0.001$) and 13.4% ($p<0.001$) as azimuth resolution decreased by 270°, 180°, 90°, 45° and 10°, respectively (Figure 16). By contrast, Ω_{LX} significantly increased as azimuth range decreased ($p<0.001$), thus showing an opposite trend compared with Ω_{APP}, most likely due to the lower azimuth segments available with reduced azimuth resolution, which limits the Ω_{LX} spatial discrimination in more restricted azimuth range. Ω_{LX} ranged from 0.74 (360°, 72 azimuth slices) to 0.94 (10°, 2 azimuth slices). Compared with the whole 360°

azimuth range, clumping index increased by 1%, 4% (p<0.001), 10% (p<0.001), 17% (p<0.001), and 28% (p<0.001), as azimuth resolution decreased by 270°, 180°, 90°, 45° and 10°, respectively (Figure 16).

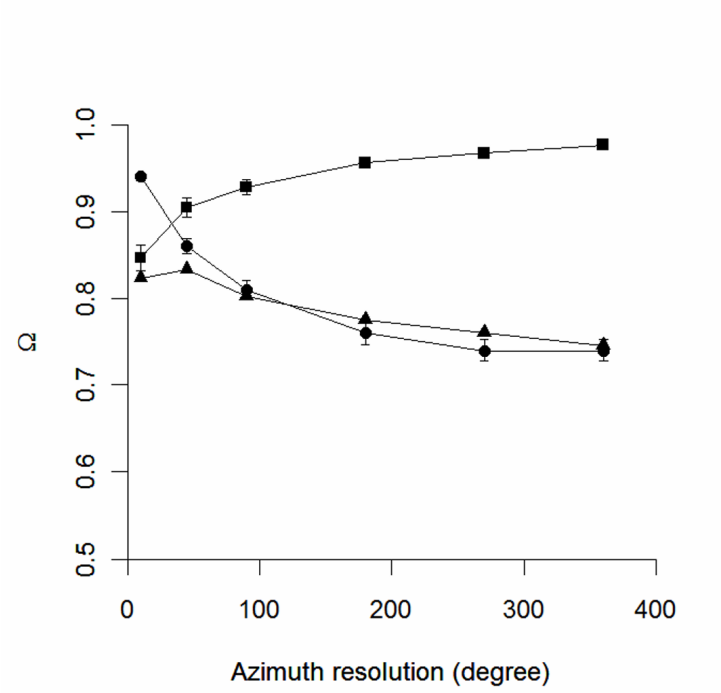

Figure 16 Foliage clumping index derived from DHP as a function of azimuth resolution. Triangles refer to true clumping index (Ω_{LT}), squares refer to Ω_{APP} derived from non segmented method and circles refer to Ω_{LX} derived from the segmented analysis of gap fraction for each ring. Standard errors are reported, with the exception of Ω_{LT}, to improve readability**.**

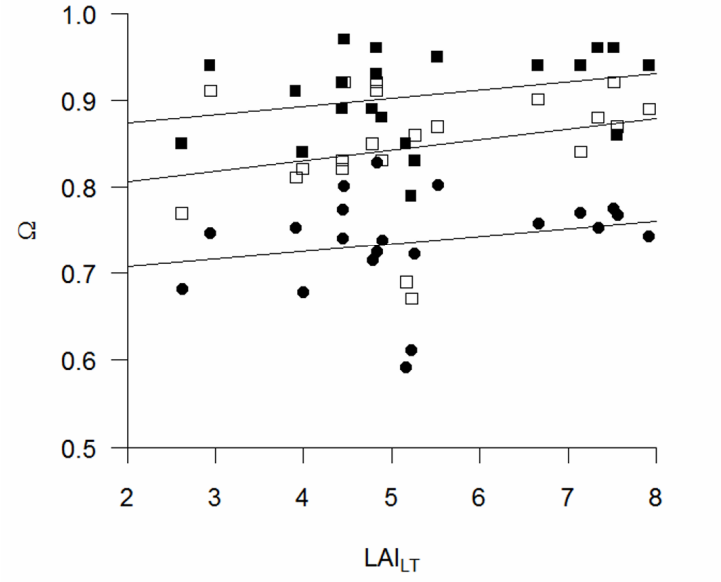

Figure 17 Foliage clumping index obtained from DHP as a function of reference leaf area index derived from littertraps (LAI_{LT}). From non segmented method, Ω_{APP} is reported from either 45° azimuth view (filled squares) and 10° azimuth view (empty squares). From segmented method, Ω_{LX} is reported from 360° azimuth view (circles).

The differences between the two log averaging methods were further analyzed by comparing Ω_{APP} and Ω_{LX} within each azimuth range considered. The analysis showed that the two clumping indices were statistically different, regardless of which azimuth resolution was considered (paired *t*-test, $p<0.001$). Both Ω_{APP} and Ω_{LX} increased as LAI_{LT} increased (Figure 17).

The different pattern observed in clumping indices derived from both gap averaging methods resulted in different leaf area index estimates from DHP. There was no difference between the results obtained from different azimuth resolution on LAI_{eff} values (ANOVA; Figure 18), therefore suggesting high homogeneity of the forest canopies sampled. By contrast, azimuth resolution significantly affected LAI_{APP} corrected for apparent clumping index (ANOVA, $p<0.001$)(Figure 18). More specifically, Tukey's test indicated that more restricted azimuth range provided largest LAI_{APP}; compared with the whole 360° azimuth range, LAI_{APP} increased by 2.4%, 4.8%, 9.9% ($p<0.001$), 14.6% ($p<0.001$) and 19.9% ($p<0.001$), as azimuth resolution decreased by 270°, 180°, 90°, 45° and 10°, respectively (Figure 18). Conversely, azimuth resolution did not show any significant influence on LAI_{LX} estimates, most likely due to the lower number of azimuth segments available with reduced azimuth view, which limits the segmented analysis in more restricted azimuth range (Figure 18).

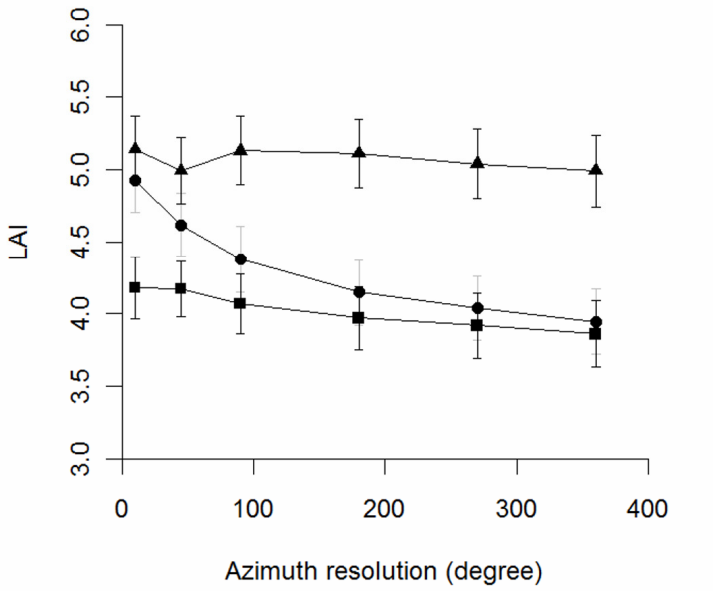

Figure 18 Leaf area index estimates derived from DHP as a function of azimuth resolution. Squares refer to effective leaf area index estimates (LAIeff), circles refer to LAI_{APP} corrected for Ω_{APP} and triangles refer to LAI_{LX} corrected for Ω_{LX}. Standard errors are reported.

Nonetheless, LAI_{LX} estimates were statistically significantly higher than LAI_{APP}, regardless of azimuth range considered (paired *t*-test, $p<0.01$), therefore indicating that Ω_{APP} only partially detect

foliage clumping, when compared to Ω_{LX}. Both LAI_{APP} and LAI_{LX} were also significantly higher than LAI_{eff} (paired *t*-test, $p<0.05$), with the exception of LAI_{eff}-LAI_{APP} paired differences obtained from 360° azimuth view.

There was a good agreement between data obtained from fisheye images using non segmented analysis and 90° view cap, and those obtained from PCA using 90° view cap (Table 7).

Table 7 RMA regression coefficients obtained from DHP, non segmented method (y-axis), and LAI-2000 PCA (x-axis) using 90° view cap. The expression used for regression was: $Y_{DHP}=aX_{PCA}$

	a	R^2	*p*
LAI_{eff}	**1,08**	0,64	0,01
LAI_{APP}	**1,10**	0,58	0,01
Ω_{APP}	**0,99**	0,52	0,01

Highlighted in bold are the slopes for which the 95% confidence intervals include one ($p<0.05$)

5.3.2 Comparison with reference values obtained by littertraps

Reference clumping index calculated from LAI_{eff} and LAI_{LT} (Ω_{LT}) for 360°, 270°, 180°, 90°, 45° and 10° azimuth range averaged 0.75 ± 0.03, 0.76 ± 0.03, 0.78 ± 0.04, 0.80 ± 0.05, 0.83 ± 0.06 and 0.82 ± 0.05, respectively (Figure 16). Ω_{LT} was found to not significantly differ with azimuth (ANOVA). Both Ω_{APP} and Ω_{LX} from DHP were compared with reference clumping (Ω_{LT}) within each azimuth range considered. Analyses revealed that Ω_{APP} was not statistically different from Ω_{LT} using 45° and 10° azimuth range, while Ω_{APP} differed in the other azimuth range (paired *t*-test, $p<0.001$). By contrast, Ω_{LX} was not statistically different from Ω_{LT}, regardless of which azimuth resolution was considered, with the exception of results obtained with the more restricted 10° azimuth view.

The leaf area index derived from either non segmented or segmented method was compared with reference LAI_{LT} derived from littertraps (Table 8) within each azimuth range considered. Results indicated that azimuth resolution did not influence greatly both LAI_{eff} and LAI_{LX}, whereas azimuth resolution showed larger influence on LAI_{APP}, with the more restricting azimuth view providing slopes closer to unity, compared with the larger azimuth view. Overall, LAI_{LX} outperformed LAI_{APP}, owing to the finest clumping correction applied in the former (Table 8).

Table 8 RMA regression coefficients of leaf area index values obtained from DHP, using either segmented or non segmented analysis of gap fraction (y-axis),and LAI_{LT} from littertraps (x-axis). The expression used for regression was: $LAI_{DHP}=aLAI_{LT}$

Azimuth	Method	*a*	R^2	*p*
360	LAI_{eff}	0.72	0.84	0.01
360	LAI_{APP}	0.74	0.84	0.01
360	LAI_{LX}	**0.93**	0.74	0.01
270	LAI_{eff}	0.73	0.82	0.01
270	LAI_{APP}	0.76	0.80	0.01
270	LAI_{LX}	**0.94**	0.71	0.01
180	LAI_{eff}	0.74	0.77	0.01
180	LAI_{APP}	0.77	0.74	0.01
180	LAI_{LX}	**0.95**	0.62	0.01
90	LAI_{eff}	0.76	0.72	0.01
90	LAI_{APP}	**0.82**	0.61	0.01
90	LAI_{LX}	**0.95**	0.53	0.01
45	LAI_{eff}	0.77	0.60	0.01
45	LAI_{APP}	**0.86**	0.41	0.01
45	LAI_{LX}	**0.93**	0.55	0.01
10	LAI_{eff}	0.78	0.71	0.01
10	LAI_{APP}	**0.91**	0.60	0.01
10	LAI_{LX}	**0.95**	0.55	0.01

Highlighted in bold are the slopes for which the 95% confidence intervals include one ($p<0.05$)

5.3.3 Foliage projection coefficient

Prior to correcting for Ω_{APP}, azimuth resolution did not influence foliage projection coefficient $G(\theta)$ from single azimuth segment approach; a nearly planophile leaf angle distribution was calculated, regardless of azimuth resolution (Figure 19). After correcting for Ω_{APP}, azimuth resolution instead showed larger influence on $G(\theta)$, with 10° azimuth resolution exhibiting a more spherical leaf angle, at least for zenith angle up to 30°(Figure 19), compared with larger azimuth resolution.

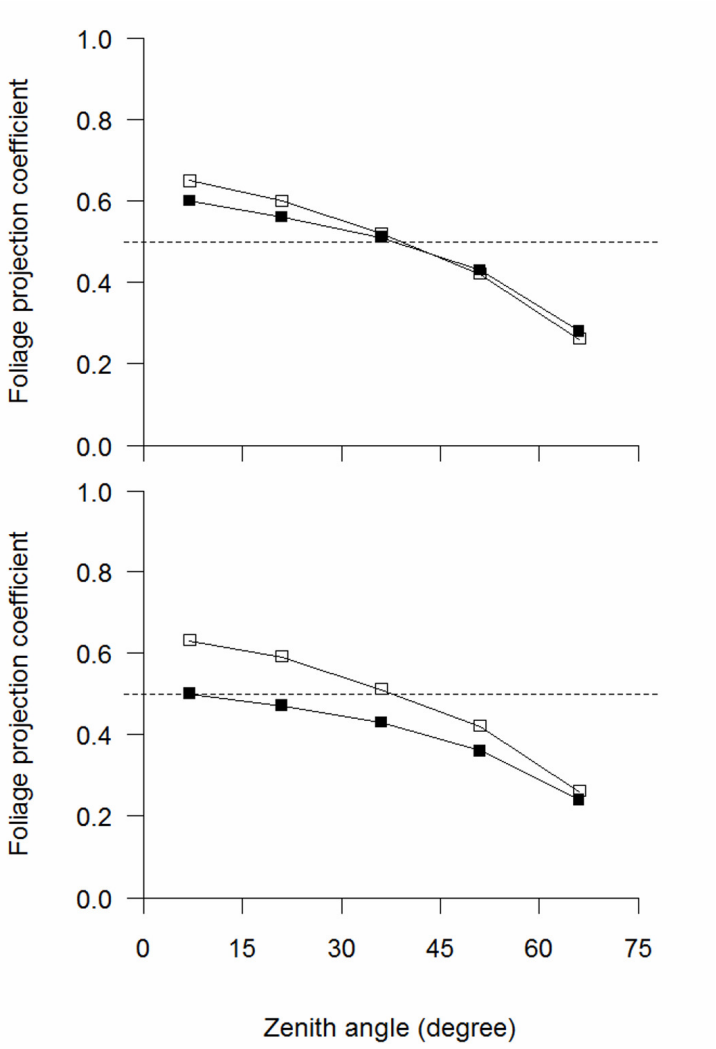

Figure 19 Foliage projection coefficient *vs* zenith angle calculated from non segmented method before (top) and after (bottom) Ω_{APP} correction for clumping. Empty squares: 360°; filled squares: 10°. The dashed lines indicate the spherical leaf angle distribution.

An opposite trend was observed for G(θ) calculated from Ω_{LX}; the G(θ) from multiple azimuth segments appeared sensitive to azimuth resolution, a results of the inherent apparent clumping correction (Figure 20). Nevertheless, after correcting for Ω_{LX}, use of restricted azimuth view, and therefore of lower number of azimuth segments, leveled the differences observed due to apparent clumping correction; nonetheless, a more vertical distribution was generally calculated after Ω_{LX} correction for clumping (Figure 20), compared with that obtained prior to Ω_{LX} clumping correction.

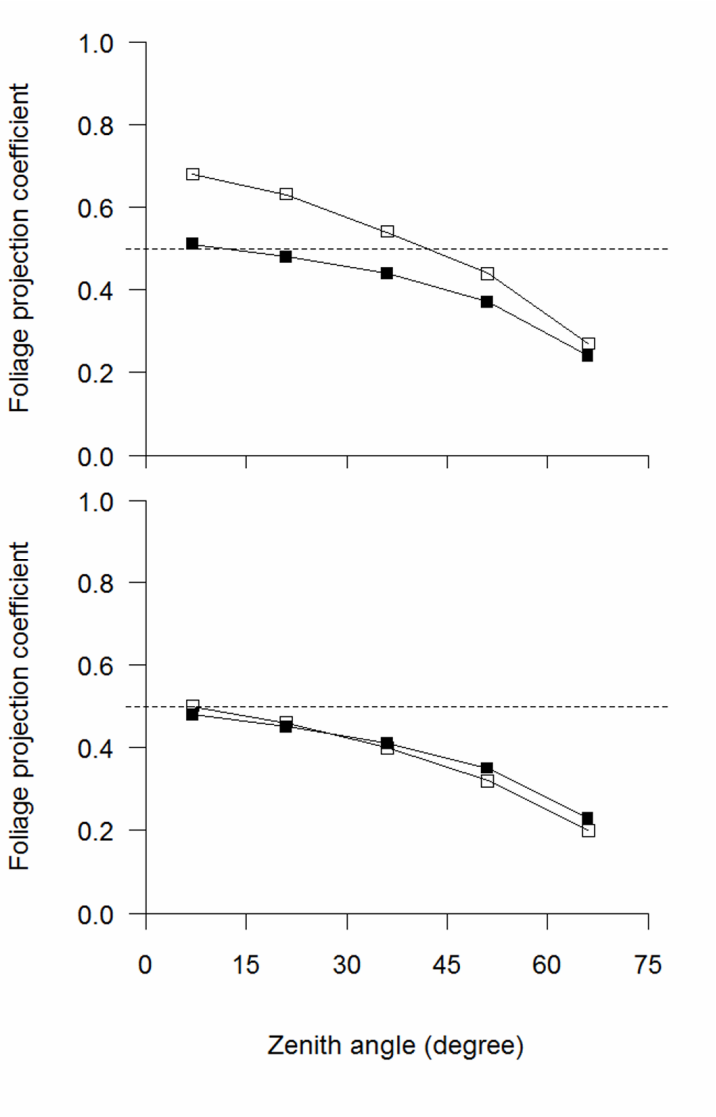

Figure 20 Foliage projection coefficient *vs* zenith angle calculated from segmented method before (top) and after (bottom) Ω_{LX} correction for clumping. Empty squares: 360°; filled squares: 10°. The dashed lines indicate the spherical leaf angle distribution.

5.4 Discussion

The study compared the performance of two different approaches for deriving foliage clumping effects in dense canopies from multiple gap fraction measurements, using a simple logarithmic gap averaging technique (Lang and Xiang 1986). Overall, results indicated that spatial resolution of canopy analysis systems influenced greatly the ability of optical method to detect and describe foliage clumping correctly, particularly regarding dense canopies, which were characterized by small scale spatial heterogeneity. This is somewhat supported by the clumping indices obtained in the current study, which appeared to increase as canopy density increased, where presumably the degree of clumping that can be detected was lower (Van Gardingen et al. 1999).

The logarithmic gap averaging technique is applied differently between non segmented and segmented method, due to different spatial scaling of logarithm averaging, and the performance of the two approaches was found to significantly differ. The non segmented method, also available in PCA, limits the spatial clumping discrimination at stand level (Ryu et al. 2010a); however, the reliability of this approach is largely dependent from azimuth resolution. Apparent clumping index decreased as azimuth resolution decreased, thus affecting LAI_{APP}, which appeared to increase as azimuth resolution decreased. Therefore, the greater clumping correction obtained at narrower views 45° and 10° improved the accuracy of corrected leaf area index estimates (LAI_{APP}), when compared with data from littertraps. The outcome was in accordance with previous studies, which showed that reliable clumping index can be found using 8-16 azimuth segments (45°-22.5° width; Leblanc et al. 2005; Macfarlane et al. 2007a; Van Gardingen et al. 1999). By contrast, LAI_{eff} values from non segmented method were found to not significantly differ as azimuth resolution varied, which indicates high stand homogeneity. Taken together, results supported reliable use of restricted view caps in PCA to derive clumping index in dense canopies, without requiring an increase in sampling intensity. On the other hand, specific problems could arise when view restrictors were applied in less dense and more heterogeneous canopies, because gap fraction is more sensitive to sampling intensity, to the orientation of caps and therefore to sky conditions. When this situation holds, use of larger azimuth cap could be appropriate to estimate LAI_{eff}. A sub sample of readings can then be collected more sparingly using narrower view caps to derive apparent clumping index. An increase of sampling in heterogeneous canopies is *a priori* recommended to achieve good spatial averaging.

The segmented analysis available in DHP can expand the applicability of the Lang and Xiang (1986) gap averaging technique, owing to its ability to divide each ring of each individual sample in multiple azimuth segments, and therefore to detect and describe the structure of clumping at sample level. Moreover, an inherent apparent clumping correction is by default calculated in HP. It is likely that the segmented method allowed higher spatial discrimination power than is possible with non segmented method. This is supported by both Ω_{LX} and LAI_{LX} calculated from segmented method, which showed best fit with reference values, compared with those obtained from non segmented method. By contrast, only LAI_{eff} available from non segmented method can be considered an effective leaf area index, which by definition must ignore any clumping compensation (Ryu et al. 2010a). As a consequence, Ω_{LX} would underestimate the true clumping index, consistently with the findings of Ryu et al. (2010a), since the numerator considered is really not an effective leaf area index.

Results from segmented method even showed that increasing the number of azimuth segments had a larger influence than use of restricted azimuth view. The more accurate Ω_{APP}

obtained restricting the azimuth range in DHP has been override by the less accurate Ω_{LX} spatial discrimination than is possible with small number of segments contained in restricted azimuth view. The outcome was in accordance with Van Gardingen et al. (1999), which showed that the optimal performance of the logarithmic gap averaging technique is obtained when each sample is segmented such that each ring had the highest number of segments whilst minimizing the total number of empty segments. This optimization can be only partially achieved in non segmented method available in PCA by averaging the light intensity at each ring over restricted azimuth range using view caps; this procedure allows a comparison of smaller portions of the canopy across the stands, compared with the whole circular 360° azimuth range, which can only partly detect the small spatial heterogeneity occurring in dense canopies; it is likely that Ω_{APP} was significantly lower than $\Omega_{LX,}$ regardless of the azimuth resolution considered..

Since the two approaches apply to DHP as well, it is recommendable to use both the procedures to estimate effective leaf area index and therefore a true clumping index. In doing so, the purpose of Ω_{APP} is to provide a way to "undo" the clumping factor compensation inherent in how PCA and DHP works, thereby allowing an independently determined clumping index calculated from segmented method to be used to compute the true clumping index.

5.5 Conclusion

Spatial variability is crucial to accurate estimation of leaf area index from indirect optical methods. This is a particularly relevant issue in dense canopies, because the resolution of canopy analysis systems is central to detect and describe canopy structure correctly (Chen et al. 1997; Ryu et al. 2010a). The main findings of the study where:

- Effective leaf area index (LAI_{eff}) from non segmented method available in PCA should be estimated using larger azimuth view, regardless of canopy density;
- The method implied in PCA can provide reliable and useful Ω_{APP} by restricting the azimuth resolution by 45° or 10°. This procedure appears particularly suitable in dense canopies, because restricted azimuth view did not require increasing sampling intensity;
- The segmented analysis in DHP incorporates apparent clumping effects. Hence, only the method available in PCA can provide LAI_{eff};
- Both the two procedures should be used in DHP, in order to provide LAI_{eff} and to discriminate clumping effect at different scales.

6. Effects of camera type on canopy properties extraction from digital photography.

6.1 Methods

6.1.1 Image collection and software analysis

The differences in camera type, namely between point and shoot camera and more recently developed digital single lens reflex camera on canopy properties retrieval from digital photography have been investigated by comparing the compact camera Nikon Coolpix 4500 (hereafter 4500) with the Digital single reflex camera Nikon D90 (hereafter D90; Figure 21).

Figure 21 Nikon D90 digital single lens reflex equipped with the Fisheye Nikkor 10.5

Cover images using both the two cameras were collected in summer 2011 and 2012. Camera setup in 4500 was configured as previously outlined in section 3.2.3. Cover images using digital single lens reflex (DSLR) were collected using an AF Nikkor 50 mm 1:1.8 D fixed lens fitted to the D90. Cover images in NEF format (RAW equivalent in Nikon) from D90 were collected during the day, under uniform sky conditions. Camera was set in aperture-priority mode, auto-focus and auto-exposure. Aperture was set to F: 8.0 and ISO 400. A D-Lighting correction (high) was applied for each image using the in-built software of the camera, or by pre-processing images with Nikon

camera software ‘Capture NX2’; this procedure provides more uniform illuminance with even better contrast between sky and non-sky pixels, thereby reducing bias from sky luminance variations across the image. Canopy properties estimations from DCP analysis were then obtained as outlined in section 4.1.1. From DCP, foliage cover (f_f), crown cover (f_c), crown porosity (□), zenithal extinction coefficient (Ω_0), LAI, with either correction for clumping (LAI CC) or without correction for clumping (LAI NC) were compared from the two cameras.

In addition, full-frame fisheye images were collected in summer 2012 with D90 using an AF Nikkor 10.5 mm 1:2.8 G fisheye lens fitted to the D90. Despite full-frame fisheye images were slightly different from circular hemispherical images, owing to the non-circular projection of the former (Figure 22), full-frame images from D90 were compared with circular fisheye images from 4500, in order to investigate the effect of camera type and image type in fisheye photography.

Full-frame fisheye images with the D90 were taken near sunset or sunrise, under diffuse sky conditions, with the camera set to ISO 400, auto-focus and Manual mode with aperture of F: 8.0, and with the shutter speed adjusted so that clear sky was over-exposed by two stops. Circular fisheye images using point and shoot Nikon Coolpix 4500 were collected as outlined in 3.2.3.

Figure 22 - Example of a full-frame fisheye image

Software image analysis in both fisheye images was performed as outlined in section 4.1.1. Both fisheye images were gamma corrected to 1.0 before software image processing in Winscanopy. Lens calibration for AF Fisheye Nikkor 10.5 was set according to Pekin and Macfarlane (2009). From fisheye (circular and full-frame) images, openness, LAI, with either LX

correction for clumping (LAI LX) or without correction for clumping (LAI NC), LX clumping index (Ω_{LX}) were compared from the two cameras.

6.1.2 Statistical analyses

The effect of site (first factor) and camera type (second factor) on canopy properties retrieval in DHP and DCP was compared using two-way ANOVA with R version 2.13.1 (R Development Core Team 2011). No interaction between site and camera type was found; hence, the interaction term was removed from the analysis.

6.2 Results

The choice of a camera influenced LAI estimates from both photographic methods; the other canopy properties retrievable from digital photography were instead not influenced by camera type (ANOVA). As regards DCP, significantly different estimates from the two cameras were obtained regarding LAI NC (Table 9). LAI NC was 6.3% smaller (two-way ANOVA, p = 0.008) while LAI CC was 3.0% smaller (two-way ANOVA, p =0.15, not significant) from 4500 than from D90 images, respectively (Figure 23).

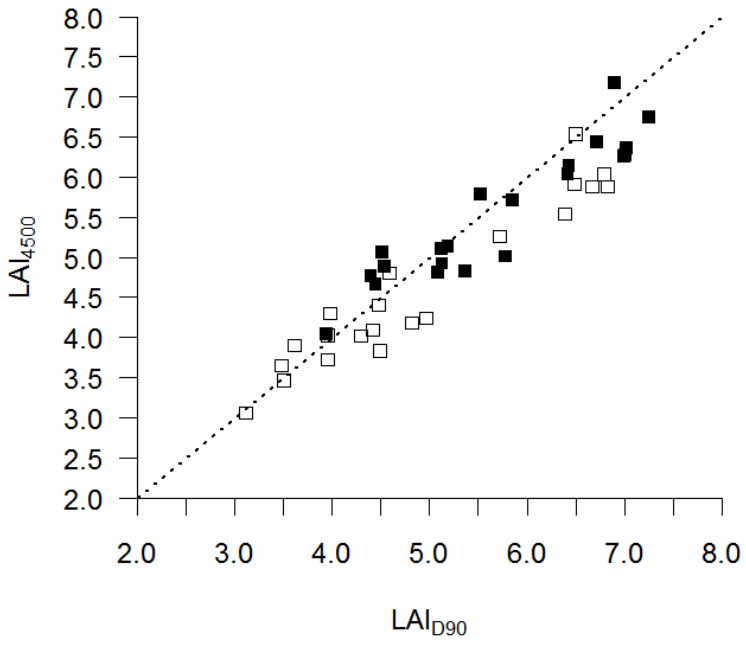

Figure 23 Comparison of leaf area index obtained from the Nikon D90 DSLR and from the Coolpix 4500 using DCP. LAI data were presented, either with CC correction for clumping (filled squares) or without correction for clumping (open squares). The dashed line indicates the 1:1 relationship between LAI NC is indicated.

Table 9 – Canopy attributes from DCP with either the 3.9 megapixel Nikon Coolpix 4500 or the Nikon D90 DSLR. Asterisks indicate means for the 4500 that significantly differed from those of the D90 (**= p<0.01). Standard errors are reported (in brackets).

Camera	f_c	f_f	φ	LAI_{NC}	LAI_{CC}	Ω_0
4500	0.93 (0.01)	0.88 (0.01)	0.06 (0.01)	4.60 (0.22)**	5.53 (0.18)	0.83 (0.02)
D90	0.94 (0.01)	0.88 (0.01)	0.06 (0.01)	4.91 (0.27)**	5.70 (0.23)	0.85 (0.02)

As regards fisheye photography, LAI values from circular fisheye photography using 4500 were significantly lower than those obtained from full-frame fisheye photography using D90 (Table 10). LAI NC was 9.9% smaller (two-way ANOVA, p = 0.005) and LAI LX was 12.2% smaller (two-way ANOVA, p = 0.003) from 4500 than from D90 fisheye images, respectively (Figure 24).

Table 10 Canopy attributes from DHP with either the 3.9 megapixels Nikon Coolpix 4500 (circular fisheye images) or the Nikon D90 DSLR (full-frame fisheye images). Asterisks indicate means for the 4500 that significantly differed from those of the D90 (**= p<0.01). Standard errors are reported (in brackets).

	Openness	LAI_{NC}	LAI_{LX}	Ω_{LX}
4500	0.05 (0.01)	3.93 (0.23)**	4.52 (0.24)**	0.86 (0.01)
D90	0.06 (0.01)	4.36 (0.36)**	5.15 (0.47)**	0.86 (0.02)

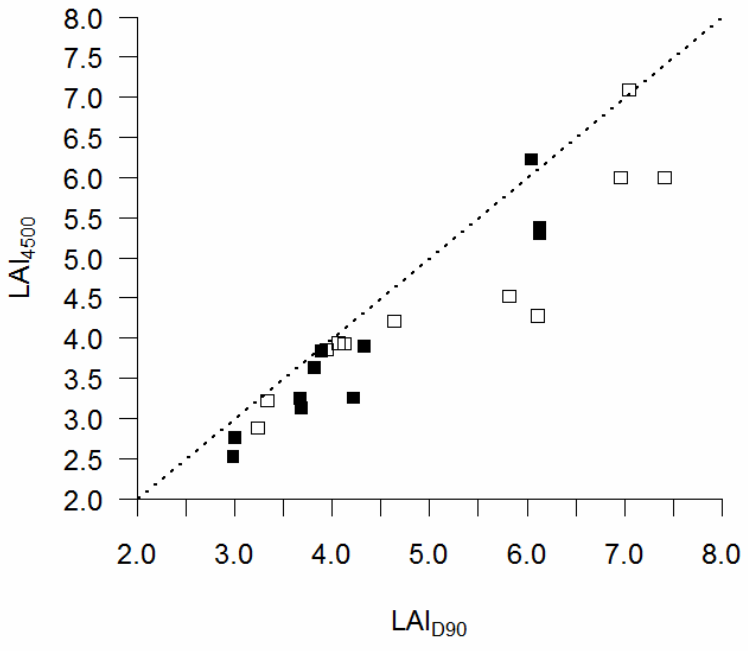

Figure 24 Comparison of leaf area index obtained from the Nikon D90 DSLR (full-frame fisheye images) and from the Coolpix 4500 (circular fisheye images) using DHP. LAI data were presented, either with LX correction for clumping (filled squares) or without correction for clumping (open squares). The dashed line indicates the 1:1 relationship between LAI NC.

The overall larger estimates of LAI obtained from both photographic methods using the DSLR camera also resulted in better agreement with reference LAI values estimated by littertraps ($LAI_{LT;}$ Table 11). LAI from D90 had slopes closer to unity and intercepts closer to zero than the corresponding LAI values from 4500. Best results from DHP were obtained when LAI values were corrected for LX clumping correction, while best results from DCP were obtained when LAI values were not corrected for clumping.

Table 11 RMA regression coefficients obtained from photography and LAI_{LT} from littertraps. The expression for regressions was: $LAI_{indirect}=a\ LAI_{LT}+b$.

Method	Correction	Camera	*a*	*b*	R^2	*p*
DHP-Circular	NC	4500	0.72	**0.18**	0.79	0.01
DHP-Circular	LX	4500	**0.77**	**0.49**	0.78	0.01
DCP	NC	4500	0.66	1.14	0.82	0.01
DCP	CC	4500	0.52	2.90	0.73	0.01
DHP-Full-frame	NC	D90	0.72	**0.38**	0.79	0.01
DHP-Full-frame	LX	D90	**0.87**	**0.57**	0.77	0.01
DCP	NC	D90	**0.82**	**0.57**	0.85	0.01
DCP	CC	D90	0.67	2.17	0.81	0.01

Highlighted in bold are intercepts for which the 95 % confidence interval includes zero, and slopes that do not significantly differ from one ($p < 0.05$)..

The differences between DCP and DHP were analyzed by comparing LAI from the two photographic methods (Table 12), despite the difficulty of comparing these different methods, owing to their extremely different field of views. Overall, DHP underestimated LAI calculated from DCP, either considering circular fisheye images from 4500 (Figure 25) or full-frame fisheye images from D90 (Figure 26). On average, underestimation was -9% ± 3% in full-frame fisheye images while it was -17% ± 2% in circular fisheye images. LAI without correction for clumping from the two photographic methods agreed better than LAI corrected for clumping, on account of the slopes closer to unity and the intercepts closer to zero of non corrected LAI values, when compared with corrected ones (Table 12).

Table 12 – RMA regression coefficients obtained from fisheye photography (y-axis) and cover photography (x-axis). The expression for regressions was: $y_{DHP}=a\ x_{DCP}+b$.

Camera	Correction	*a*	*b*	R^2	*p*
4500	NC	**1.04**	-0.85	0.88	0.01
4500	C	1.39	-3.19	0.81	0.01
D90	NC	**0.85**	**0.26**	0.91	0.01
D90	C	1.25	-1.83	0.97	0.01

Highlighted in bold are intercepts for which the 95 % confidence interval includes zero, and slopes that do not significantly differ from one ($p < 0.05$). C refers to LAI corrected for Chen and Cihlar correction for clumping in cover photography, while C refers to Lang and Xiang correction for clumping in fisheye photography.

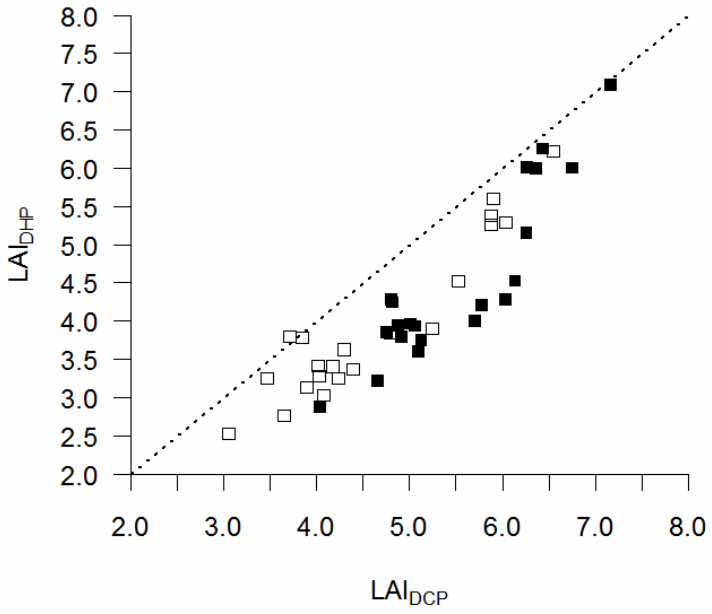

Figure 25 Comparison of leaf area index calculated from circular DHP with leaf area index calculated from DCP using the Coolpix 4500. LAI from DHP using the LX correction for clumping was compared with LAI from DCP after CC correction for clumping (filled squares). LAI without correction (LAI NC) for clumping was also compared between the two methods (open squares). The dashed line indicated the 1:1 relationship between LAI NC.

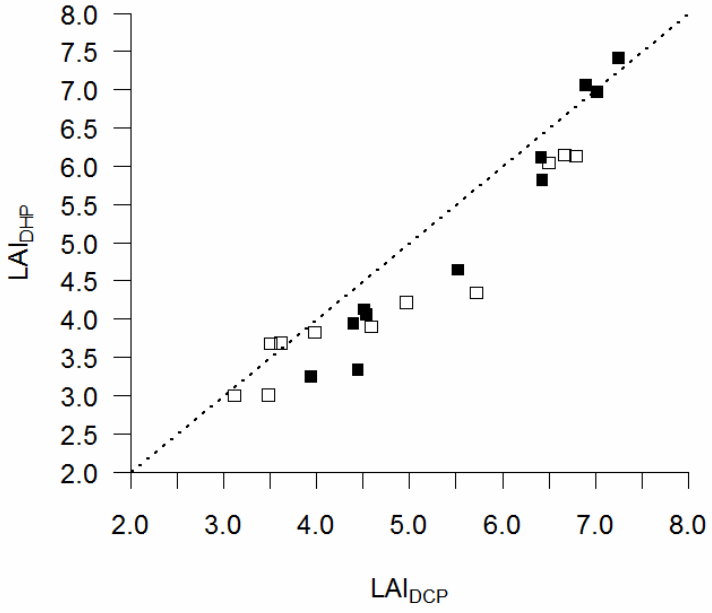

Figure 26 Comparison of leaf area index calculated from full-frame DHP with leaf area index calculated from DCP using the Nikon D90. LAI from DHP using the LX correction for clumping was compared with LAI from DCP after CC correction for clumping (filled squares). LAI without correction (LAI NC) for clumping was also compared between the two methods (open squares). The dashed line indicated the 1:1 relationship between LAI NC.

The differences between DHP and DCP were further analyzed by comparing foliage and crown cover from DCP and canopy closure (1-openness) from DHP, despite the fact the two measures were not directly comparable (see also Figure 2, page 19).

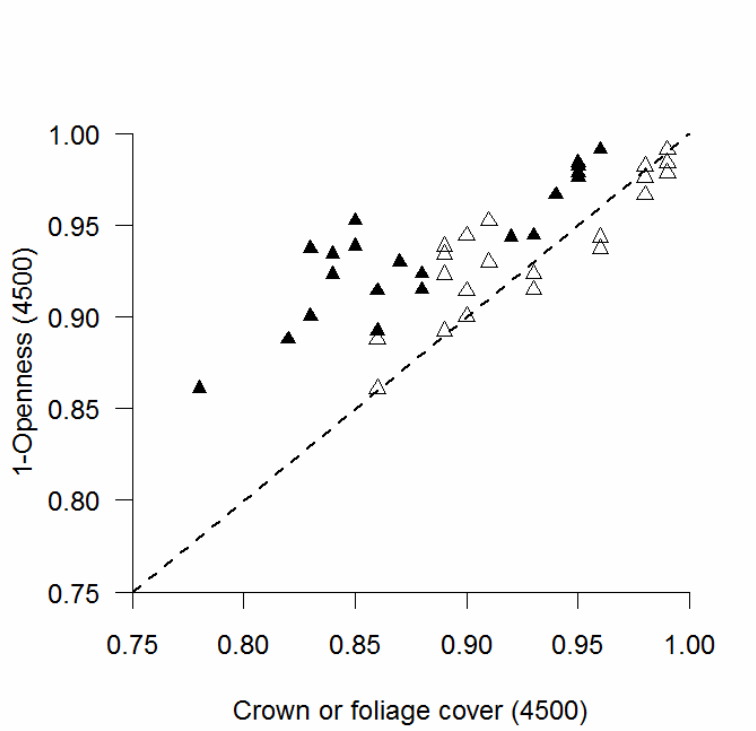

Figure 27 Comparison of canopy closure (1-openness) calculated from DHP and either foliage cover (filled triangles) or crown cover (empty triangles) from DCP using the Coolpix 4500. The dashed line indicates the 1:1 relationship between canopy closure and crown cover.

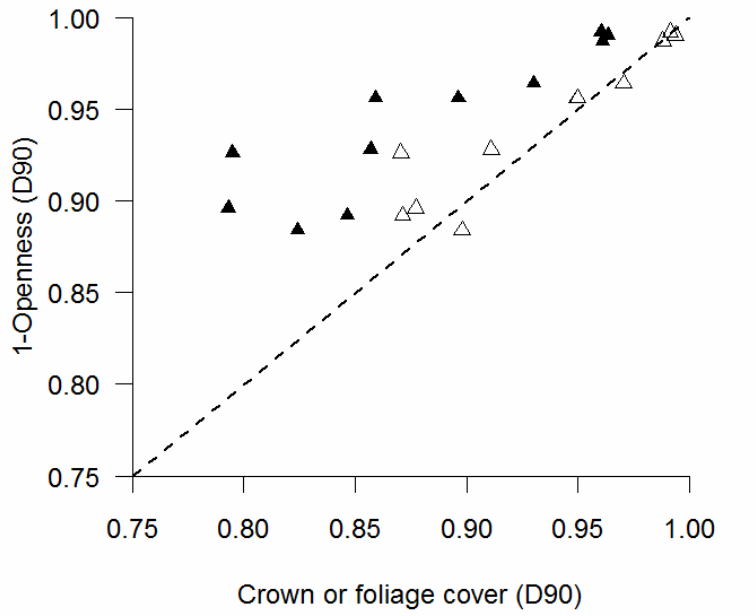

Figure 28 Comparison of canopy closure (1-openness) calculated from DHP and either foliage cover (filled triangles) or crown cover (empty triangles) from DCP using the Nikon D90. The dashed line indicates the 1:1 relationship between canopy closure and crown cover.

In plots with $f_c > 0.9$ there was good agreement between crown cover from DCP and canopy closure from DHP using 4500 (Figure 27); LAI from the two methods also agreed well in these plots. In plots with $f_c < 0.9$ there was poorer agreement between the two methods. Similar result was obtained using Nikon D90 (Figure 28).

6.4 Discussion and conclusions

The choice of a camera did affect LAI estimates from both fisheye photography and DCP. DSLR camera produced larger estimates of LAI, which also resulted in better agreement with direct LAI measurements obtained by littertraps. Given that thorough appraisals of digital photographic methods using DSLR cameras are still rare, and generalization over canopy measurement procedures using DSLR cameras are therefore hardly feasible, results of the study allowed reliable use of camera setup and processing procedures applied in the current study.

The difference in DCP was statistically significant only in LAI NC values, although the discrepancy between the two camera outputs were rather small (~6%). Slightly larger and significant differences (~11%) were found regarding fisheye photography. However, larger differences were quite expected because full-frame fisheye images have better image resolution than the corresponding circular fisheye images used in 4500, regardless of pixel resolution. Full-frame images have a reduced field of view, such that the zenithal range of 0-90° extends to the corners of the rectangular images, providing more pixels in the analyzed canopy and sky regions than circular images. As such, it is reasonable to infer that the influence of higher quality cameras on canopy estimates from DHP would be lower than observed in the current study. Nevertheless, a previous comparison of full-frame fisheye images between Nikon Coolpix 4500 and DSLR Nikon D80 in less dense canopies (LAI~2) showed slightly larger differences from the two cameras, with LAI values from 4500 being 12-15% smaller than those from D80 images (Pekin and Macfarlane 2009). Hence, the performance of the two cameras may differ more in sparse and heterogeneous canopies.

DHP underestimated LAI, when compared with DCP. The underestimation appeared lower using D90, probably because full-frame fisheye images have better image resolution than the corresponding circular fisheye images, being most comparable with DCP. LAI NC from the two photographic methods agreed better than LAI corrected for clumping, probably because of the different clumping corrections applied in the two photographic methods. A comparison of the CC clumping correction in the two methods have not been carried out because the CC correction is better suited in DCP, whose higher resolution may result in better ability to separate large between-crowns gaps from small within-crown gaps in DCP, when compared with DHP; hence, a

comparison of CC clumping correction in the two methods would be necessarily disadvantageous to fisheye photography, especially in dense canopies.

The best agreement between crown cover from DCP and canopy closure from DHP was achieved in stands where crown cover was above 0.9. Although the two measures were not directly comparable, it is reasonable to infer the number of images collected may have been insufficient and biased at the sites where canopies were less homogeneous (crown cover was less than 0.9), and the resulting differences in LAI from the two photographic methods were higher.

In summary, results supported use of high quality DSLR cameras for estimating forest leaf area, on account of the best accuracy obtained with DSLR, compared with the point-and-shoot Nikon Coolpix 4500. The differences should be attributed largely from the better quality of the optics in the two cameras. The lowest differences observed in DCP using the two cameras, however, suggested that canopy analysis in this high resolution imagery method would be less sensitive to quality lenses than DHP.

7. Conclusive considerations

The research provides a thorough technical appraisal of available existing digital photographic techniques for forest canopy properties estimation. Overall, results indicated the reliability of digital photographic methodology. Digital photography can greatly expand the number of field sample measurements that are possible, as compared with other canopy instrumentations, cutting down the cost of the instrumentation needed. Moreover, photography is a permanent record of canopy structure (Rich et al. 1999), which can be repeatedly analyzed to retrieve several distinct canopy attributes. Images can also be reprocessed when improved models become available and used to perform other measurements, for example, fractal dimension, architecture and understory light (Jonckheere et al. 2004). In addition, canopy photography holds great promise as the current advancements in digital technology, resulting in better quality of lenses and higher spatial radiometric resolution of cameras, combined with advanced digital image analysis techniques, are bringing canopy photography to a mature stage, where both field methods and post-processing of images will be soon regarded as strength rather weakness in comparison with other methods (Macfarlane 2011).

The study compared hemispherical photography, a technique which has already proven to be a powerful method for measuring canopy structure and forest light regime (Jonckhhere et al. 2004), with alternative photographic methods. In particular, the most recent cover photography holds great promise as a means to quickly obtain inexpensive estimates of forest canopy properties over large areas, being therefore highly suitable for routine, research and monitoring of forest canopy estimates (Macfarlane et al. 2007c). Although DCP was originally developed for sparse to moderately dense broadleaf forests, the current study demonstrated the high accuracy of the method in very dense forest, in which the ability to detect small gaps in crowns resulted in more accurate gap fraction retrieval near the zenith than is possible with fisheye sensors (Pekin and Macfarlane 2009). In addition to being a very simple, rapid and accurate method, DCP provided a suite of various important canopy attributes such as crown porosity, crown and foliage cover. These attributes should expand the applicability of canopy properties to other ground-based research fields such as phenological studies, plant pathology and forest inventory. Moreover, the DCP would be the ideal ground-based method for plot-scale calibration and testing of remote sensing methods; for example, vertical FOV remote sensing can potentially provide estimates of cover that can be compared directly with those obtained from DCP (Pekin and Macfarlane 2009).

A comparison of logarithm gap fraction averaging procedures implied in DHP provided the opportunity to define an operational method to derive effective leaf area index and apparent clumping index from non segmented method; the procedure was also easily applicable to LAI-2000 PCA. Combining both the segmented and non segmented methods in DHP allowed discriminating different spatial scaling of clumping index. The results have important implications for the evaluation of satellite-based leaf area index product of airborne laser scanning (LiDAR). In fact, some LiDAR derived effective leaf area mapping used $-\overline{\ln P_0(\theta)}$ instead of using $-\ln \overline{P_0(\theta)}$, which incorporated clumping effects. Accordingly, it is recommendable to use the $-\ln \overline{P_0(\theta)}$ method to calculate effective leaf area index, which is the first step to estimate true leaf area index in the protocols of canopy structure measurement (Ryu et al. 2010a). Finally, the spatial variation of clumping indices would be useful to evaluate coarse resolution of global clumping index map and improve land surface models (Ryu et al. 2010a).

Last, but not least, the study tested and defined standardized field protocol for image acquisition and software analysis in both compact and digital single lens reflex cameras, which may assist to greatly improve canopy photography, in order to achieve the standards of an ideal device. The study also provided a suite of several variables of interest, which can provide insights towards the characterization of deciduous forests, and that can be further applied for further canopy studies in deciduous stands.

References

Amiro BD, Chen JM, Liu J 2000. Net primary productivity following forest fire for Canadian ecoregions. Can. J. Forest Res. 30: 939-947.

Amorini E, Bruschini S, Manetti MC 1998. La sostenibilità della produzione legnosa di qualità del ceduo di castagno: modello alternativo al ceduo a turno breve.In:Comunità Montana Prealpi Trevigiane (Ed.), Atti del Convegno nazionale sul castagno, Cison di Valmarino (Tv), 23-25 Ottobre 1997, 217-230.

Amorini E, Fabbio G, Bertini G 2009. Dinamica del ceduo oltre turno e avviamento ad alto fusto dei cedui di faggio. Risultati del protocollo "Germano Gambi" sull'Alpe di Catenaia (Arezzo). Annali CRA – Centro di Ricerca per la Selvicoltura 36: 151-172.

Anderson MC 1964. Studies of the woodland light climate I. The photographic computation of light condition. Journal of Ecology 52: 27-41.

Anderson MG 1966. Stand structure and light penetration II. A theoretical analysis. Journal of Applied Ecology 3: 41-54.

Anderson MC 1971. Radiation and crop structure. In: Sestak, Z., Catsky, J., Jarvis, P.G., (eds.) Plant photosynthetic Production Manual of Methods. Junk, the Hague: 77-90.

Anderson MC 1981. The geometry of leaf distribution in some south-eastern Australian forests. Agricultural Forest Meteorology 25:195-205.

Barclay HJ 1998. Conversion of total leaf area to projected leaf area in lodgepole and Douglas-fir. Tree Physiology 18: 185-193.

Bolstad PV, Gower ST 1990. Estimation of leaf area index in fourteen southern Wisconsin forest stands using a portable radiometer. Tree Physiol. 7: 115-124.

Bonhomme R, Varlet-Grancher C, Chartier M 1974. The use of hemispherical photographs for determining the leaf area index of young crops. Photosynthetica 8: 299-301.

Bréda N 2003. Ground-based measurements of leaf area index: a review of methods instruments and current controversies. J. Exp. Bot. 54: 2403–2417.

Brown MJ, Parker GG 1994. Canopy light transmittance in a chronosequence of mixed-species deciduous forests. Can. J. For. Res. 24: 1694-1703.

Campbell GS 1986. Extinction coefficients for radiation in plant canopies calculated using an ellipsoidal inclination angle distribution. Agric. For. Meteorol.: 36: 317-321.

Canham CD, Denslow JS, Platt WJ, Runkie JR, Spies TA, White PS 1990. Light regimes beneath closed canopies and tree-fall gaps in temperate and tropical forests. Can. J. For. Res. 20: 620-631.

Cannell MGR, Milne R, Sheppard LJ, Unsworth MH 1987. Radiation interception and productivity of willow. J. Appl. Ecol. 24: 261-278.

Cescatti A 2007. Indirect estimates of canopy gap fraction based on the linear conversion of hemispherical photographs. Methodology and comparison with standard thresholding techniques. Agric. For. Meteorol. 143: 1-12.

Chan SS, McCreight RW, Walstad JD, Spies TA 1986. Evaluating forest vegetative cover with computerized analysis of fisheye photographs. Forest Science 32: 1085-1091

Chen JM, Black TA 1992. Defining leaf area index for non-flat leaves. Plant Cell Environ. 15: 421-529.

Chen JM, Black TA, Adams RS 1991. Evaluation of hemispherical photography for determining plant area index and geometry of a stand. Agric. For. Meteorol. 56: 129-132.

Chen JM, Cihlar J 1995. Quantifying the effect of canopy architecture on optical measurements of leaf area index using two gap size analysis methods. IEEE T. Geosci. Remote Sens. 33: 777-787.

Chen J.M. Rich P.M. Gower S.T. Norman J.M. Plummer S. 1997. Leaf area index of boreal forests: Theory techniques and measurements. J. Geophys. Res. 102 29429-29443.

Chianucci F, Cutini A 2012. Digital hemispherical photography for estimating forest canopy properties: current controversies and opportunities. iForest 5: 290-295.

Comeau PG, Braudmandl TF, Xie CY, 1993. Effects of overtopping vegetation on light availability and growth of Engelmann spruce (*Picea engelmannii*) seedlings. Can. J. For. Res. 23: 2044-2048.

Cutini A 1996. The influence of drought and thinning on leaf area index estimates from canopy transmittance method. Ann. Sci. For. 53: 595-603.

Cutini A 2001. New management options in chestnut coppices: an evaluation on ecological bases. For. Ecol. Manage. 141: 165-174.

Cutini A 2003. Litterfall and leaf area index in the CONECOFOR permanent monitoring plots. Journal of Limnology 61: 62-68.

Cutini A, Chianucci F, Giannini T 2009. Effetto del trattamento selvicolturale su caratteristiche della copertura, produzione di lettiera e di seme in cedui di faggio in conversione. Annali CRA – Centro di Ricerca per la Selvicoltura: 109-124.

Cutini A, Matteucci G, Mugnozza GS 1998. Estimation of leaf area index with the Li-Cor LAI 2000 in deciduous forests. Forest Ecol. Manage.: 105 55-65.

De Wit CT 1965.Photosynthesis of Leaf Canopies. Agricultural Reports No. 663. PUDOC, Wageningen, the Nederlands.

Dufrêne E, Bréda N 1995. Estimation of deciduous forest leaf area index using direct and indirect methods. Oecologia 104: 156-162.

Englund SR, O'Brie JJ, Clark DB 2000. Evaluation of digital and film hemispherical photography for predicting understorey light in a Bornean tropical rain forest. Agric. For. Meteorol. 97: 129-139.

Evans GD, Coombe DE 1959. Hemispherical and woodland canopy photography and the light climate. Journal of Ecology 47: 103-113.

Frazer GW, Canham CD, Lertzman KP 1999. Gap light analyzer (GLA) Version 2.0: Imaging software to extract canopy structure and gap light transmission indices from true-color fisheye photographs user's manual and program documentation. Burnaby BC Canada: Simon Fraser University, pp.36.

Frazer GW, Fournier RA, Trofymow JA, Hall RJ 2001. A comparison of digital and film fisheye photography for analysis of forest canopy structure and gap light transmission. Agric. For. Meteorol. 109: 246-263.

Gendron F, Messier C, Comeau P 1998. Comparison of various methods for estimating the mean growing season percent photosynthetic photon flux density in forests. Agric. For. Meteorol. 92: 55-70.

Grace J 1987. Theoretical ratio between 'one-sided' and total surface area for pine needles. Forest Science 17: 292-296.

Hill R 1924. A lens for whole sky photographs. Quarterly Journal of the Royal Meteorological Society 50: 227-235.

Inoue A, Yamamoto K, Mizoue N, Kawahara Y 2004. Effects of image quality, size and camera type on forest light envrionment estimates using digital hemispherical photography. Agric. For. Meteorol. 126: 89-97.

Jarčuška B 2008. Methodological overview to hemispherical photography demonstrated on an example of the software GLA. Folia Oecologica 35: 66-69.

Jarčuška B, Kucbel S, Jaloviar P 2010. Comparison of output results from two programmes for hemispherical image analysis: Gap Light Analyser and WinScanopy. Journal of Forest Science 56 (4): 147-153.

Jarvis PG, Leverenz JW 1983. Productivity of temperate deciduous and evergreen forests. In: Lange O.L. Nobel P.S. Osmond C.B. Ziegler H. (Eds.) Physiological Plant Ecology IV. Encyclopedia of Plant Physiology Vol. 12D, Springer-Verlag, New York, pp. 233-280.

Jennings SB, Brown ND Sheil D 1999. Assessing forest canopies and understorey illumination: canopy closure, canopy cover and other measures. Forestry 72: 59-74.

Jensen JLWV (1906). Sur les fonctions convexes et les inégalités entre les valeurs moyennes. Acta Mathematica 30 (1): 175–193

Johansson T 1989. Irradiance within the canopies of young trees of European aspen (*Populus tremula*) and European birch in stands of different spacing. Forest Ecol. Manag. 28: 217-236.

Jonckheere I, Fleck S, Nackaerts K, Muys B, Coppin P, Weiss M, Baret F, 2004. Review of methods for in situ leaf area index determination: Part I. Theories sensors and hemispherical photography. Agric. For. Meteorol. 121: 19-35.

Jonckheere I, Nackaerts K, Muys B, Coppin P, 2005. Assessment of automatic gap fraction estimation of forests from digital hemispherical photography. Agric. For. Meteorol. 132: 96–114.

Kucharik CJ, Norman JM, Murdock LM, Gower ST 1997. Characterizing canopy nonrandomness with a multiband vegetation imager (MVI). J. Geophys. Res. 102: 29455-29473.

Kucharick CJ, Norman JM, Gower ST 1998. Measurement of branch area and adjusting leaf area index from indirect measurements. Agric. For. Meteorol. 11(91): 69-88.

Kucharik CJ, Norman JM, Gower ST 1999. Characterization of radiation regimes in non-random forest canopies: theory, measurements, and a simplified modelling approach. Tree Physiology 19: 695-706.

Lang ARG, McMurtrie RE, Benson ML 1991. Validity of surface area indices of Pinus radiata estimated from transmittance of the sun's beam. Agric. For. Meteorol. 57: 157-170.

Lang ARG, Xiang Y 1986. Estimation of leaf area index from transmission of direct sunlight in discontinuous canopies. Agric. For. Meteorol. 35: 229–243.

Leblanc SG 2002. Correction to the plant canopy gap-size analysis theory used by the tracing radiation and architecture of canopies instrument. Appl. Opt. 41: 7667–7670.

Leblanc SG, Chen JM, Fernandes R, Deering DW, Conley A 2005. Methodology comparison for canopy structure parameters extraction from digital hemispherical photography in boreal forests. Agric. For. Meteorol. 129: 187-207.

Leblanc S 2008. DHP-TRACWin Manual. Natural Resource Canada. Canada Centre for Remote Sensing, Saint-Hubert, Québec, Canada.

Lebourgeois F, Bréda N, Ulrich E, Granier A 2005. Climate-growth relationships of European beech (*Fagus sylvatica* L.) in the French Permanent Plot Network (RENECOFOR). Trees 19: 385-401.

Lowman MD, Nadkarni NM (eds) 1995. Forest canopies. Academic, New York, 322 pp.

Macfarlane C 2011. Classification method of mixed pixels does not affect canopy metrics from digital images of forest overstorey. Agric. For. Meteorol.: 151 833-840.

Macfarlane C, Arndt S, Livesley SJ, Edgar AC, White DA, Adams MA, Eamus D 2007a. Estimating of leaf area index in eucalypt forest with vertical foliage using cover and fullframe fisheye photography. Forest Ecol. Manag. 242: 756-763.

Macfarlane C, Grigg A, Evangelista C 2007b. Estimating forest leaf area using cover and fullframe fisheye photography: Thinking inside the circle. Agric. For. Meteorol. 146: 1-12.

Macfarlane C, Hoffman M, Eamus D, Kerp N, Higginson S, McMurtrie R, Adams MA 2007c. Estimation of leaf area index in eucalypt forest using digital photography. Agric. For. Meteorol.143: 176–188.

Meier IC, Leuschner C 2008. Leaf size and Leaf Area Index in *Fagus sylvatica* Forests: Competing Effects of Precipitation Temperature and Nitrogen Availability. Ecosystems 11: 655-669

Messier C, Puttonen P 1995. Spatial and temporal variation in the light environment of developing Scots pine stands: the basis for a quick and efficient method for characterizing light. Can. J. For. Res. 25: 343-354.

Miller J 1967. A formula for average foliage density. Australian Journal of Botany 15: 141-144.

Monsi M, Saeki T 1953. The light factor in plant communities and its significance for dry matter production. Japanese Journal of Botany 14: 22-52.

Myneni R, Nemani R, Running S 1997. Estimation of global leaf area index and absorbed par using radiative transfer models. IEEE T. Geosci. Remote 35: 1380-1393.

Nilson T 1971. A theoretical analysis of the frequency of gaps in plant stands. Agric. For. Meteorol. 8: 25-38.

Norman JM, Campbell GS 1989. Canopy structure. In: Pearcy RW, Ehleringer JR, Mooney HA, Rundel PW eds. Plant physiological ecology: field methods and instrumentation. London: Chapman and Hall: 301-325.

Parent S, Messier C 1996. A simple and efficient method to estimate microsite light availability under a forest canopy. Can. J. For. Res. 26: 151-154.

Pekin B, Macfarlane C 2009. Measurement of Crown Cover and Leaf Area Index using Digital Cover Photography and its application to Remote Sensing. Remote Sens. 1: 1298-1320.

Pierce LL, Running SW 1988. Rapid estimation of coniferous forest leaf area index using a portable integrating radiometer. Ecology 69: 1762-1767.

Pisek J, Ryu Y, Alikas K 2011. Estimating leaf inclination and G-function from leveled digital camera photography in broadleaf canopies. Trees 25: 919-924.

R Development Core Team 2011. R: A language and environment for statistical computing. R Foundation for Statistical Computing Vienna (Austria).

Rich PM, Wood J, Vieglais DA, Burek K, Webb N (1999). HemiView Manual Revision Number: 2.1. Delta-T Devices, Ltd.

Ross J 1981. The Radiation Regime and Architecture of Plant Stands. Junk The Hague, pp. 391.

Ryu Y, Nilson T, Kobayashi H, Sonnentag O, Law BE, Baldocchi DD 2010a. On the correct estimation of effective leaf area index: Does it reveal information on clumping effects? Agric. For. Meteorol. 150: 463-472.

Ryu Y, Sonnentag O, Nilson T, Vargas R, Kobayashi H, Wenk R, Baldocchi DD 2010b. How to quantify tree leaf area index in an open savanna ecosystem: a multi-instrument and multi-model approach. Agric. For. Meteorol. 150: 63-76.

Sampson DA, Allen HL 1995. Direct and indirect estimates of Leaf Area Index (LAI) for lodgepole and loblolly pine stands. Trees 9: 119-122.

Sellin A 2000. Estimating the needle area from geometric measurements: application of different calculation methods to Norway spruce. Trees 14: 215-222.

Smith NJ 1991. Predicting radiation attenuation in stands of Douglas-fir. For. SCI 37: 1213-1223.

Smith ER, Ritters KH 1994. A comparison of forest canopy transmittance estimators. Can. J. For. Res. 24:

Smith FW, Sampson DA, Long JN 1991. Comparison of leaf area index estimates from tree allometrics and measured light interception. For. Sci. 37: 1682-1688.

Thimonier A, Sedivy I, Schleppi P 2010. Estimating leaf area index in different types of mature forest stands in Switzerland: a comparison of methods. Eur. J. Forest Res. 129: 543-562.

Van Gardingen PR, Jackson GE, Hernandez- Daumas S, Russell G, Sharp L 1999. Leaf area index estimates obtained for clumped canopies using hemispherical photography. Agric. For. Meteorol. 94 : 243-257.

Vansereven JP 1969. Recherches sur l'écosysteème foret. Série B: La chenaie mélangée calcicole de Virelles-Blaimont. Contribution n.30 : L' index foliaire et sa measure par photoplanimétrie. Bull. Soc. R. Bot. Belg. 102: 373-385.

Wagner S 1998. Calibration of grey values of hemispherical photographs for image analysis. Agr. For. Meteor. 90: 103-117.

Wang YS, Miller DR 1987. Calibration of the hemispherical photographic technique to measure leaf area index distributions in hardwood forests. Forest Science 33: 110-126.

Warren-Wilson 1960. Inclined point quadrats. New Phytol. 59: 1-7.

Warren-Wilson 1963. Estimation of foliage denseness and foliage angle by inclined point quadrats. Aust. J. Bot. 11: 95-105.

Warton DI, Wright IJ, Falster DS, Westoby M 2006. Bivariate line-fitting models for allometry. Biol. Rev. 81: 259–291.

Watson DJ 1947. Comparative physiological studies in the growth of field crops. I. Variation in net assimilation rate and leaf area between species and varieties, and within and between years. Ann. Bot. 11: 41-76.

Weiss M, Baret F, Smith GJ, Jonckheere I, Coppin P 2004. Review of methods for in situ leaf area index (LAI) determination. Part II. Estimation of LAI, errors and sampling. Agric. For. Meteorol. 121: 37-53.

Welles JM, Norman JM 1991. Instrument for indirect measurement of canopy architecture. Agronomy Journal 83: 818-825.

Zhang Y, Chen JM, Miller JR 2005. Determining digital hemispherical photograph exposure for leaf area index estimation. Agric. For. Meteorol. 133: 166–181.

Zhongguo MA, Chen X, Guli J, Chang C 2009. Study on LAI estimation of broadleaf forests in arid areas using digital hemispherical photography: the Tarim River Basin China. Journal of Environmental Technology and Engineering 2009 2(3):106-111.

ANNEX 1

In chapter 5, two different gap averaging methods are presented, which were used to derive LAI from logarithm of gap fraction [P(θ)]:

$$-\left[\ln \overline{P(\theta)}\right] \tag{28}$$

$$-\left[\overline{\ln P(\theta)}\right] \tag{29}$$

Equation (28) derives LAI from logarithm of arithmetic mean of gap fraction, while equation 29 calculates LAI from arithmetic mean of logarithms, which equals the logarithm of the geometric mean of gap fraction . In fact:

$$\ln\left[\left(\prod_{1}^{n} P(\theta)\right)^{1/n}\right] = \frac{1}{n}\sum_{1}^{n} \ln P(\theta) = \left[\overline{\ln P(\theta)}\right] \tag{30}$$

In mathematics, the inequality of arithmetic and geometric means states that the arithmetic mean of a list of non-negative real numbers is greater than or equal to the geometric mean of the same list; and further, that the two means are equal if and only if every number in the list is the same. This inequality can be proven via finite form of Jensen's inequality (Jensen, 1906).

Jensen's finite form:

For a real convex function φ, numbers x_1, x_2, ..., x_n in its domain$_i$, Jensen's inequality can be stated as:

$$\varphi\left(\frac{\sum x_i}{n}\right) \leq \frac{\sum \varphi(x_i)}{n} \tag{31}$$

and the inequality is reversed if φ is concave, which is:

$$\varphi\left(\frac{\sum x_i}{n}\right) \geq \frac{\sum \varphi(x_i)}{n} \tag{32}$$

For instance, the function -log(x) is convex, so substituting $\varphi(x) = -\log(x)$ in the previous formula (31) establishes the (logarithm of) the familiar arithmetic mean-geometric mean inequality:

$$-\ln\left(\frac{x_1 + x_2 + \ldots + x_n}{n}\right) \leq -\ln\left[\sqrt[n]{x_1 x_2 \cdot \cdots x_n}\right] \tag{33}$$

Since LAI_{eff} is derived through eq. 28 and true leaf area index corrected for either Ω_{APP} (LAI_{APP}) or Ω_{LX} (LAI_{LX}) is derived through eq. 29, the Jensen's inequality indicated that:

$$LAI_{eff} \leq LAI_{APP};\ LAI_{eff} \leq LAI_{LX} \tag{34}$$

Moreover, since LAI_{APP} can also be expressed as the logarithm of the arithmetic mean of the gap fraction averaged for a number of segments for each ring (eq. 28; segmented method), whilst LAI_{LX} is based on the logarithm of the geometric mean of the gap fraction averaged for a number of segments for each ring (eq. 29; segmented method), the Jensen's inequality also indicate that:

$$LAI_{eff} \leq LAI_{APP} \leq LAI_{LX} \quad (35)$$